



# รายงานวิจัยฉบับสมบูรณ์

โครงการ ความต้านทานต่อการสึกหรอแบบขัดสีของเหล็กหล่อโครเมียมสูงประเภทไฮโป ยูเทคติกที่มีปริมาณโครเมียมร้อยละ 26 โดยมวลที่ผสมโมลิบดินัม

โดย นายสุดสาคร อินธิเดช และคณะ

# รายงานวิจัยฉบับสมบูรณ์

โครงการ ความต้านทานต่อการสึกหรอแบบขัดสีของเหล็กหล่อโครเมียมสูงประเภทไฮโปยูเทคติกที่ มีปริมาณโครเมียมร้อยละ 26 โดยมวลที่ผสมโมลิบดินัม

# คณะผู้วิจัย

- 1 ผู้ช่วยศาสตราจารย์ สุดสาคร อินธิเดช
- 2 รองศาสตราจารย์ประสงค์ ศรีเจริญชัย
- 3 Professor Yasuhiro Matsubara

# สังกัด

มหาวิทยาลัยมหาสารคาม จุฬาลงกรณ์มหาวิทยาลัย

Kurume National College of

Technology

สนับสนุนโดยสำนักงานคณะกรรมการอุดมศึกษา สำนักงานกองทุนสนับสนุนการวิจัยและมหาวิทยาลัยมหาสารคาม (ความเห็นในรายงานนี้ของผู้วิจัย สกอ. และ สกว. ไม่จำเป็นต้องเห็นด้วยเสมอไป)

# บทคัดย่อ

เหล็กหล่อไฮโปยูเทคติคที่มีปริมาณโครเมียม 26% โดยมวลที่เติมโมลิบดีนัม 0-3% ได้ถูกเตรียมขึ้นเพื่อ ศึกษาความต้านทานการสึกหรอแบบขัดสี ได้ทำการอบอ่อนขึ้นงานที่อุณหภูมิ 1173 K เป็นเวลา 18 ks และทำการ ชุบแข็งขึ้นงานที่อุณหภูมิ 1323 K และจากนั้นอบคืนตัวที่อุณหภูมิสามระดับระหว่าง 673 ถึง 823 K เป็นเวลา 7.2 ks ได้แก่ อุณหภูมิที่ให้ความแข็งสูงที่สุด ( $H_{Tmax}$ ), อุณหภูมิต่ำกว่าอุณหภูมิที่ให้ความแข็งสูงที่สุด ( $H_{Tmax}$ ) ทำการประเมินผลความต้านทานการสึกหรอแบบขัดสีโดย ใช้การทดสอบการสึกหรอแบบขัดสีแบบ Suga abrasive wear test และการทดสอบการสึกหรอแบบขัดสีเดย ในท์เหลือค้าง ( $V_{\gamma}$ ) ในขึ้นงานที่ผ่านกรรมวิธีทางความร้อนแปรผันตามปริมาณโมลิบดีนัมและเงื่อนไขของกรรมวิธีทางความร้อน ความสัมพันธ์เชิงเส้นระหว่างน้ำหนักที่สูญเสียและระยะทางเป็นเส้นตรงในทุกขึ้นงาน อัตราการสึกหรอ (Rw) ต่ำที่สุดเกิดขึ้นในขึ้นงานทั้งในสภาพชุบแข็งและในขึ้นงาน  $H_{Tmax}$  ทั้งสองวิธีทดสอบ ค่า Rw ในการทดสอบการสึกหรอแบบ Suga abrasive wear test จะมากกว่าในการทดสอบการสึกหรอแบบล้อยางภายใต้ สภาวะเดียวกัน ค่า Rw สูงที่สุดในขึ้นงาน L- $H_{Tmax}$ หรือ  $H_{Tmax}$  นอกจากนี้ยังพบว่าค่า Rw ลดลงตามความแข็งที่ เพิ่มขึ้น ค่า Rw ต่ำที่สุดในขึ้นงานที่มีปริมาณออสเตนในต์เหลือค้าง 10-15 เปอร์เซ็นต์โดยปริมาตร ค่า Rw ลดลงตามปริมาณโมลิบดีนัมที่เพิ่มขึ้นในการทดสอบการสึกหรอแบบ Suga abrasive wear test และ Rw ลดลงเล็กน้อย เมื่อปริมาณโมลิบดีนัมเพิ่มขึ้นในการทดสอบการสึกหรอแบบ Suga abrasive wear test และ Rw ลดลงเล็กน้อย เมื่อปริมาณโมลิบดีนัมที่เพิ่มขึ้นในการทดสอบการสึกหรอแบบ Suga abrasive wear test และ Rw ลดลงเล็กน้อย เมื่อปริมาณโมลิบดีนัมที่เพิ่มขึ้นในการทดสอบการสึกหรอแบบ Suga abrasive wear test และ Rw ลดลงเล็กน้อย เมื่อปริมาณโมลิบดีนัมที่เพิ่มขึ้นในการทดสอบการสึกหรอแบบขัดสีล้อยาง

**คำหลัก**: เหล็กหล่อโครเมียมสูง 26% Cr, กรรมวิธีทางความร้อน, ความแข็ง, ออสเตนไนต์เหลือค้าง, ความต้านทาน ต่อการสึกหรอแบบขัดสี, ผลของ Mo

**Abstract** 

Hypoeutectic 26 wt% Cr cast irons with 0-3 wt% Mo were prepared in order to investigate

their abrasive wear behavior. The annealed test pieces were hardened from 1323 K and then

tempered at three levels of temperatures between 673 and 823 K for 7.2ks, the temperature giving

the maximum hardness ( $H_{Tmax}$ ), lower temperature than that at  $H_{Tmax}$  (L- $H_{Tmax}$ ) and higher

temperature than that at H<sub>Tmax</sub> (H-H<sub>Tmax</sub>). The abrasive wear resistance was evaluated using Suga

wear test (two-body-type) and Rubber wheel wear test (three-body-type). It was found that

hardness and volume fraction of retained austenite  $(V\gamma)$  in the heat-treated specimens varied

depending on the Cr and Mo contents. A linear relation was obtained between wear loss and wear

distance. The lowest wear rate  $(R_W)$  was obtained in both the as-hardened and  $H_{Tmax}$  specimens.

The highest R<sub>W</sub> was mostly obtained in the H-H<sub>Tmax</sub> specimens. Under the same heat treatment

condition, the R<sub>W</sub> in Suga wear test was much greater than that in Rubber wheel wear test. The R<sub>W</sub>

decreased with increasing the hardness. The lowest R<sub>W</sub> obtained in the specimen with a certain

amount of retained austenite, 10-15% $V_{\gamma}$ . The Rw decreased with increasing Mo content in Suga

abrasive test and it decreased little by Mo addition in Rubber wheel wear test.

**Keywords:** 26% Cr cast iron, heat treatment, hardness, retained austenite, abrasive wear

resistance, Mo effect

# **Executive Summary**

งานวิจัยนี้มีจุดมุ่งหมายเพื่อศึกษาความต้านทานต่อการสึกหรอแบบขัดสีของเหล็กหล่อโครเมียมสูง 26% Cr ที่เติมธาตุผสมโมลิบดินัม (Mo) โดยได้เลือกปริมาณโมลิบดินัมในช่วง 0-3% ซึ่งใช้งานอย่างกว้างขวางในโรงงาน อุตสาหกรรมปูนซีเมนต์ อุตสาหกรรมเหมืองแร่ อุตสาหกรรมผลิตเหล็กกล้าและอุตสาหกรรมผลิตกระแสไฟฟ้าใน ประเทศไทย โดยมีช่วงกำหนดระยะเวลาในการดำเนินการตามสัญญาคือ 15 มิถุนายน 2554-15 มิถุนายน 2556 และมีการดำเนินงานวิจัยโดยสรุปดังนี้

การดำเนินงานต่างๆได้ดำเนินการเสร็จสิ้นก่อนแผนที่กำหนดไว้เป็นเวลาหนึ่งปีโดยได้มีการปรับเปลี่ยน ขอบเขตการทำวิจัยบางส่วนตามคำแนะนำของนักวิจัยที่ปรึกษาของผู้รับทุน เนื่องจากเป็นงานวิจัยต่อเนื่องจากการ รับทุนวิจัยก่อนหน้านี้ (MRG5180110) ทำให้สามารถทำวิจัยแล้วเสร็จก่อนกำหนด ผู้รับทุนวิจัยได้ดำเนินการทำวิจัย ตามคำแนะนำของนักวิจัยที่ปรึกษาจนเสร็จสมบูรณ์และมีผลงานตีพิมพ์ ดังนั้นจึงสามารถประเมินได้ว่าประสบ ความสำเร็จและบรรลุจุดประสงค์ของโครงการ

ตลอดระยะเวลาดำเนินการผู้รับทุนได้มีโอกาสโดยได้สร้างความร่วมมือกับกลุ่มวิจัยทั้งในและต่างประเทศ นอกจากนี้ยังได้รับความร่วมมือจากทางภาคอุตสาหกรรมทั้งในและต่างประเทศ จึงมั่นใจว่าจะสามารถวิจัยต่อยอด และผลิตผลงานวิจัยเกี่ยวกับการปรับปรุงความต้านทานการสึกหรอของเหล็กหล่อโครเมียมสูงเพื่องานด้านการขัดสี ต่อไปได้โดยอาศัยศักยภาพของผู้รับทุน นักวิจัยที่ปรึกษา และหน่วยงานต่างๆทั้งภายในและนอกประเทศ

ผู้รับทุนได้ผลิตผลงานวิจัย 3 ผลงาน โดยอยู่ในรูปการนำเสนอผลงานในที่ประชุมวิชาการระดับชาติ 1 ผลงาน ประชุมวิชาการระดับนานาชาติ 1 ผลงานและอยู่ระหว่างการส่งผลงานเพื่อตีพิมพ์ในวารสารวิชาการระดับ นานาชาติ (Material Transaction ประเทศญี่ปุ่น ซึ่งมี Impact factor ปี 2011 เท่ากับ 0.779 ) จำนวน 1 ผลงาน ซึ่งคาดว่าน่าจะสามารถตีพิมพ์ในเดือนสิงหาคมปี 2555 นี้ และจะส่งผลงานการตีพิมพ์ฉบับสมบูรณ์ให้กับ ทางโครงการต่อไป

# Acknowledgements

ผู้วิจัยขอขอบพระคุณ สำนักงานคณะกรรมการอุดมศึกษา สำนักงานกองทุนสนับสนุนงานวิจัยและ มหาวิทยาลัยมหาสารคามเป็นอย่างสูงที่ได้ให้ทุนสนับสนุนการวิจัยเพื่อทำการวิจัยในครั้งนี้ และขอขอบคุณ หน่วยงานต่างๆต่อไปนี้ที่ได้ให้ความอนุเคราะห์เครื่องมือและให้ความร่วมมือในการวิจัยโครงการนี้เป็นอย่างดีดังนี้

- 1. คณะวิศวกรรมศาสตร์ มหาวิทยาลัยมหาสารคามสำหรับอุปกรณ์และสถานที่ในการทำวิจัย
- 2. นายอรรถสิทธิ์ ชูประจง ภาควิชาวิศวกรรมโลหการ คณะวิศวกรรมศาสตร์ จุฬาลงกรณ์มหาวิทยาลัย สำหรับความช่วยเหลือในการทดสอบการสึกหรอแบบล้อยาง
- 3. Professor Nobuya Sasaguri and Professor Kaoru Yamamoto, Cast Metal Research Laboratory, Kurume National College of Technology, Japan สำหรับการวิเคราะห์หาปริมาณ ออสเตนในต์เหลือค้าง
- 4. Kawara steel Co. Ltd., Japan และ บริษัทพนาพลัสจำกัด สำหรับความอนุเคราะห์อุปกรณ์ในการ เตรียมชิ้นงานทดสอบ
- 5. แผนกเครื่องมือ บริษัทไทยปาร์กเกอร์ไรซิ่งจำกัด สำหรับเครื่องทดสอบ SEM

ผศ. สุดสาคร อินธิเดช รศ. ประสงค์ ศรีเจริญชัย Professor Yasuhiro Matsubara

# Content

	Page
Chapter 1 Introduction	8
Chapter 2 Literature Survey	13
Chapter 3 Experimental Procedure	42
3.1 Preparation of specimen	42
3.2 Heat treatment procedure	44
3.3 Observation of microstructure	45
3.4 Hardness measurement	45
3.5 Measurement of volume fraction of retained austenite	45
3.6 Abrasive wear test	52
<b>Chapter 4 Experimental Results and Discussions</b>	54
4.1 Characterization of test specimen	54
4.2 Suga abrasive wear test	59
4.3 Rubber wheel abrasive wear test	67
4.4 Mechanism of abrasive wear	75
Chapter 5 Conclusions	77
References	78
Output	82
Appendix	83

#### **Chapter 1**

#### Introduction

#### 1.1 Background

Alloyed white cast irons containing 15-30 mass% Cr (hereafter shown by %) have been employed as abrasion wear resistant materials for more than 50 years. The microstructures of these alloys consist of hard eutectic carbides and strong matrix structure providing the excellent wear resistance and suitable toughness. It is well known that 15% to 20% Cr cast irons have been commonly used for rolling mill rolls in the steel plants, while cast irons with 25% to 28% Cr have been applied to rollers and tables of pulverizing mills in the mining and cement industries. High Cr cast irons with hypocutectic composition are preferable than those with hypereutectic composition because they are free from precipitation of massive primary carbides that reduce the toughness. [1]

In the hypoeutectic cast iron, as-cast microstructure consists of primary matrix and eutectic M<sub>7</sub>C<sub>3</sub> carbide. Austenite which is stable at high temperature under an equilibrium condition will transform to ferrite and carbides or pearlite on the way of cooling. Under non-equilibrium condition, however, the austenite may remain stable or partially transforms to pearlite or martensite depending on the chemical composition and the cooling rate. [1,2] Austenite is favored by high cooling rate, high Cr/C ratio and additions of alloying elements such as Ni, Cu and Mo. [1-3] The supersaturation of Cr and C in austenite decreases the martensite start temperature (Ms), and resultantly, the austenite could be remained even at room temperature.

Austenite has high toughness and it can be work-hardened to increase the surface hardness during service, but is limited to the spalling wear resistance. Improved service performance could be obtained by heat treatment and addition of some alloying elements to provide martensitic matrix with higher wear resistance. In the most cases, a suitable martensitic matrix produced by heat treatment used to provide an increase of abrasion wear resistance. To obtain a martensitic matrix, the cast iron is held in austenite region at 900-1100 °C to enable secondary carbide

precipitation in austenite (so-called as destabilization of austenite) and followed by fan air cooling to room temperature. The precipitation of secondary carbides in the matrix during heat treatment must be related to the wear resistance and somewhat to the mechanical properties. [4] The retained austenite should be normally limited less than 5 vol% by single or multiple tempering to avoid the spalling during service. [1,3] In practical applications of high Cr cast iron, adequate heat treatment must be given to the cast iron to get optimal combination of the hardness and the toughness which is mainly controlled by quantity of retained austenite. Since quantitative measurement of retained austenite for high Cr cast iron has been performed successfully by X-ray diffraction method [5-8], it is possible to connect the wear resistance and other properties with the amount of retained austenite.

The purpose of alloy addition is to suppress the formation of pearlite in the as-cast condition and to improve the hardenability in the post heat treatment. Since Cr is presented in both the eutectic and secondary carbides, the rest of Cr is retained in the matrix to suppress the pearlite transformation and increase the hardenability. Therefore, the supplementary addition of the third alloying elements such as Mo, Ni, Cu are needed to harden the matrix fully. [1] The effect of additional alloying element to high Cr cast iron has been extensively reported. [2-4,6,9-19] It was reported that the highest hardness after heat treatment of 26% Cr cast iron was obtained by Mo addition. [3] This is because Mo can form its special carbide of Mo<sub>2</sub>C or M<sub>2</sub>C type with extremely high hardness as eutectic and secondary carbides, and this lead to improve the wear resistance. [11]

The abrasive wear is a type of wear that is brought about by means of hard particles. Moreover, these particles act to concentrate the stress, leading to operate a plastic deformation in the matrix on the surface of the cast iron. The wear rate which is measured by the wear loss depends on several factors, microstructure, kind of abrasive particle, type of relative or mutual movements, chemical reaction and temperature. [1] Abrasive wear results in a high cost for annual replacement in mining, ore treatment, cement and other industries.

Abrasive wear may be divided into two types; two-body type and three-body type. [20] In the two-body type abrasive wear process, the wear takes place when the hard angular abrasive particles contact the wear surface, e.g., hammer and liner of impact crusher. The local stresses between abrasive particles and wear surface are high enough to crush the particles, leading up to the heavy plastic deformation on the wear surface. As the wear progresses, the tips of particles are fixed on the wear surface, and the matrix is removed first. In this case, therefore, the high surface hardness enough to resist the penetration of particles and the sufficient toughness enough to resist cracking are required. In order to evaluate the two-body type abrasive wear, an abrasive paper, which is made by high hardness abrasive particles such as SiC or Al<sub>2</sub>O<sub>3</sub> fixed on the paper by a glue, are generally used. Suga wear tester is suitable to evaluate the two-body type abrasive wear resistance.

In the three-body type abrasive wear, the wear environment consists of two counter materials and abrasive particles. The stress in this case is lower than that in the case of two-body type abrasion wear. The stress is not high enough to crush the abrasive particles. It occurs in the application where moving particles come freely into wearing surfaces. Typical applications involving this type of wear are for ball and rod mills, pulverizers, like vertical mill and roll crushers. [21] The toughness of materials composed for these surroundings do with to be smaller than that composed for the two-body type abrasion and is likely obtained by the materials as hard as possible. The suitable wear testing machine for three-body type abrasion wear is a Rubber Wheel wear tester where SiO<sub>2</sub> particles are used as the abrasives.

Many laboratory tests have been carried out to evaluate the abrasion wear resistance of high Cr cast irons. However, the test data did not often validly to simulate correctly the wear behavior occurred in the industrial applications. Therefore, it is considered that the systematic and detailed studies on the abrasive wear behavior are necessary. Particularly, the systematic investigation of Mo addition to the heat-treated high Cr cast irons on the wear behavior is much more important.

There are many researches on the wear resistance of high Cr cast irons [4,7,8,11], and recently a study on the heat treatment behavior of hypoeutectic high Cr cast iron with various Mo contents has been reported. [3] The abrasive wear behavior of heat-treated hypoeutectic 16% Cr cast iron with different Mo content was studied by the previous work. [7,8] However, the research

on the abrasion wear behavior of heat-treated hypoeutectic 26% Cr cast iron containing molybdenum using two-body type and three-body type wear testers has not been investigated.

In this study, hypoeutectic 26% Cr cast irons varying Mo content were prepared and they were heat-treated. Then, two types of abrasion wear tests, Suga abrasion wear test and Rubber Wheel abrasion wear test, are conducted. The relationships between abrasion wear, hardness, volume fraction of retained austenite ( $V_{\gamma}$ ) and molybdenum content are investigated. In addition, the wear behaviors are discussed in connection with the matrix structure in the cast iron.

#### 1.2 Objective of Research

To clarify the effects of Mo content on heat treatment characteristics, hardness, volume fraction of retained austenite  $(V_{\gamma})$  and matrix structure, and finally the relations between such parameters and wear resistance, two-body type and three-body type abrasive wear tests were carried out.

#### 1.3 Scopes of Research

- 1.3.1 To heat-treat specimens by annealing, hardening and tempering at 3 levels tempearture.
- 1.3.2 To measure the hardness.
- 1.3.3 To measure the volume fraction of retained austenite  $(V_{\gamma})$ .
- 1.3.4 To investigate the behavior of abrasive wear using Suga abrasion wear test and Rubber Wheel abrasion wear test.
- 1.3.6 To observe the microstructure by Optical Microscope (OM) and Scanning Electron Microscope (SEM).
- 1.3.7 To discuss the effects of hardness, volume fraction of retained austenite  $(V_{\gamma})$  and Mo content on abrasive wear resistance.

# 1.4 Advantages of Research

- 1.4.1 This research reveals the characteristics in two-body and three-body type abrasion wear of 26% Cr cast iron with different Mo content.
- 1.4.2 This research clarifies the relationship between hardness, volume fraction of retained austenite  $(V_{\gamma})$  and abrasive wear resistance.
- 1.4.3 This research clarifies the effect of heat treatment condition and Mo content on abrasive wear resistance.
- 1.4.4 These data are keenly profitable for practical heat treatment to improve wear resistance of 26% Cr cast iron with Mo

#### Chapter 2

#### **Literature Survey**

High Cr cast irons with hypoeutectic composition are commonly used as abrasion wear resistant materials. The 15-30% Cr cast irons are popular as the cast irons for abrasive wear resistance. The alloys containing 25-28% Cr have been especially developed for materials with abrasion and corrosion resistance. The high Cr cast irons are generally used with austenitic or martensitic matrix. The purpose of Mo addition is to suppress the transformation of pearlite in the as-cast state and to improve the hardenability during subsequent heat treatment.

In the mining industry, the life of parts and components of machines are subjected to the services conditions in which the materials are received. They are mainly abrasion wear and impact stress. It is well known that the abrasive wear is very severe during operation. Therefore, the improvement of wear resistant materials contributes to not only the reduction of cost but also that of downtime and the time of maintenance. The performance of high Cr cast iron depends on the function of microstructure, material properties, abrasion wear resistance, corrosion resistance and etc. Although the high Cr cast irons with hypo- and hypereutectic compositions have been used, the hypoeutectic irons have been used mainly as the components. The research and development of microstructure of cast iron has been done from the viewpoint of alloying and processing. The main challenge was the studies on carbide structure, such as volume fraction, size and morphology of carbides, alloying and solidification. The improvement of the matrix structure has been carried out through subsequent thermal process so-called heat treatment.

#### 2.1 Solidification and Microstructure of High Chromium Cast Iron

High Cr cast irons are based on Fe-C-Cr system. Alloying elements such as Mo, Ni and Mn are usually added to the cast iron. The chemical compositions of several cast irons for abrasion resistance are shown in Table 2.1.

Table 2.1 Chemical composition of abrasion wear resistance cast irons. [10]

Class	Туре	Designation	С	Mn	Si	Ni	Cr	Мо	P	S	Cu
I	Α	Ni-Cr-HC	2.8-3.6	2.0	0.8	3.3-5.0	1.4-4.0	1.0	0.3	0.15	-
	В	Ni-Cr-LC	2.4-3.0	2.0	0.8	3.3-5.0	1.4-4.0	1.0	0.3	0.15	-
	C	Ni-Cr-GB	2.5-3.7	2.0	0.8	4.0	1.0-1.5	1.0	0.3	0.15	-
	. D	Ni-HiCr	2.5-3.6	2.0	2.0	4.5-7.0	7.0-11.0	1.5	0.1	0.15	-
П	A	12% Cr	2.0-3.3	2.0	1.5	2.5	11.0-14.0	3.0	0.1	0.06	1.2
	В	15%Cr-Mo	2.0-3.3	2.0	1.5	2.5	14.0-18.0	3.0	0.1	0.06	1.2
	D	20%Cr-Mo	2.0-3.3	2.0	1.0-2.2	2.5	18.0-23.0	3.0	0.1	0.06	1.2
Ш	A	25%Cr	2.3-3.3	2.0	1.5	2.5	23.0-30.0	3.0	0.1	0.06	1.2

LC = low carbon, HC = high carbon, GB = graphite bearing

The solidification of high Cr cast irons have been studied by many researchers. [6,9-15,17,22-29] Thorpe and Chicco [22] constructed the liquidus surface phase diagram of Fe-Cr-C system using accurate experimental technique and high purity materials, and it is as shown in Fig. 2.1. The majority of chemical composition of commercial cast iron for abrasion wear resistance is 12-30% Cr and 2.0-3.6% C. In the hypoeutectic cast irons, the microstructure consists of primary austenite ( $\gamma_p$ ) and eutectic structure of austenite ( $\gamma_E$ ) and carbides. The reaction is described as followed,

$$L \rightarrow \gamma_E + M_7 C_3$$
 or  $\gamma_E + (CrFe)_7 C_3$ 

Although most of high Cr cast iron finishes solidifying completely within the eutectic region, a quasi-peritectic at low temperature may be occur if liquid remains after the eutectic reaction. This reaction is described as follow,

$$M_7C_3 + L \rightarrow M_3C$$

The  $M_3C$  carbides appear at the shell of  $M_7C_3$  carbide as intervening between  $M_7C_3$  carbide and liquid. The high Cr cast irons with hypereutectic composition are generally used as hard facing alloy being added by some strong carbide formers.

In the range of less than 10% Cr, eutectic of γ and M<sub>3</sub>C carbide is precipitated as follows,

$$L \rightarrow \gamma + M_2 C$$

The crystal lattice of  $M_7C_3$  carbide is hexagonal, whereas the  $M_3C$  carbide is orthorhombic. The hardness of  $M_7C_3$  carbide is 1400-1800 HV and it is much harder than that of  $M_3C$  carbide with 800-1100 HV. [6] As Cr content increases, the eutectic line moves to high temperature and low C sides, and therefore, the C content in austenite decreases. From Fig. 2.1, the eutectic carbon content in 12% Cr cast iron is about 4.0% while for 30% Cr cast iron is around 2.8%.

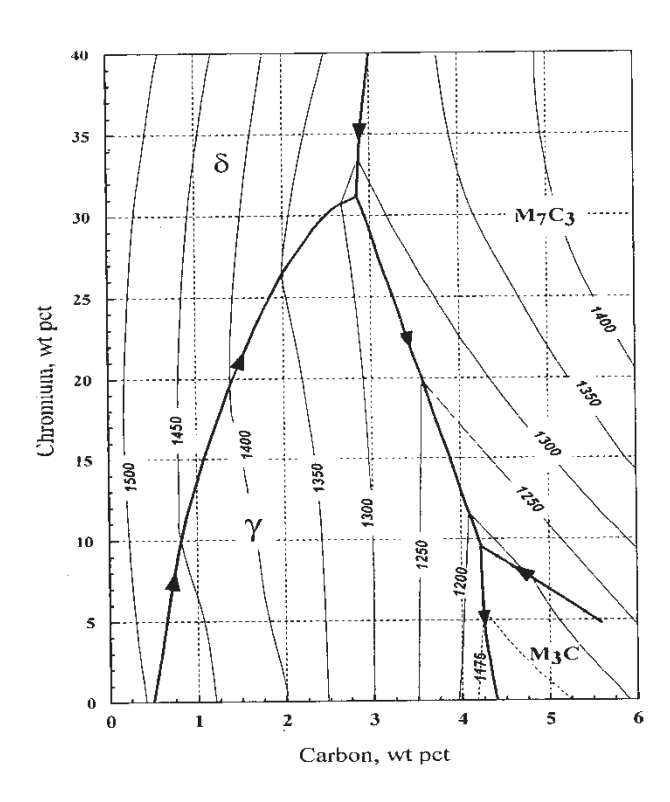


Fig. 2.1 Liquidus surface phase diagram of Fe-Cr-C system. [22]

Generally, the wear resistance and the mechanical properties of high Cr cast iron depend on the type, morphology and that distribution of carbides on matrix structure. [1] In hypocutectic cast iron, the eutectic is randomly nucleated in the liquid after solidification of primary austenite dendrite, and then grows with a cellular interface to solidify as a colony structure. The eutectic carbides develop in rod-like shape and the rods of carbide join together to form an interconnected colony structure with lamella cross-section. [2]

The rod-like  $M_7C_3$  carbides become finer with increasing the Cr content and the rate of solidification. In addition, the size of eutectic colony is also decreased and the carbide spacing is also reduced with an increase in the Cr content and rate of solidification. G. Powell observed the

carbide morphology of high Cr cast iron by SEM and reported that both the rod-like and blade-like of M<sub>7</sub>C<sub>3</sub> carbides in the white cast iron with Cr content more than 12% were not completely discontinuous but interconnected. [13] Dogan found that the eutectic colony in eutectic cast iron contains completely rod-like M<sub>7</sub>C<sub>3</sub> carbides, whereas the hypoeutectic and hypereutectic high Cr cast irons have both rod-like and blade-like carbides. [14] It was found that slower growth rates (smaller undercooling) favored to solidify in the morphology of blade-like carbides, whereas faster growth rates (larger undercooling) favored that of the rod-like carbides. Volume fraction of carbide can be calculated as a function of the carbon and chromium contents of the alloy. Maratray [16] demonstrated the following equations,

$$V_C = 12.33x\%C + 0.55x\%Cr - 15.2$$

From the equation,  $V_C$  increases with an increase in C and Cr contents. Laird suggested that it needs caution if this equation is availed because of limited accuracy. [27] Dupin found that there is some the difference in the  $V_C$  between the surface and core regions of the casting. [23]

The carbides morphology is closely related to the fracture toughness. The high fracture toughness is obtained in the cast iron with fine eutectic carbide. In order to refine the eutectic carbide, the rapid cooling has been used to increase the nucleation of carbide and to suppress the growth of carbide. By contrast, slow cooling results in larger dendrite arm spacing and coarser the eutectic carbides. [17]

Alloy addition has been used to modify the carbide structure. Boron additions of 0.1-0.3% decreased the solubility of carbon in austenite and increased the number of carbide nuclei. As a result, it produced a large number of fine carbides in as-cast structure. [30] The effect of V on the eutectic colony size was investigated by Y. Matsubara and et al. [28] It was reported that V reduces the eutectic freezing range and the size of eutectic carbides as well as that of eutectic colony is refined.

As introduced earlier, matrix structure is very important factor affecting the abrasive wear resistance. In hypoeutectic cast iron, the as-cast matrix consists of primary austenite dendrites and eutectic of as example shown in Fig. 2.2. [6] The austenitic matrix was obtained in the 26% Cr

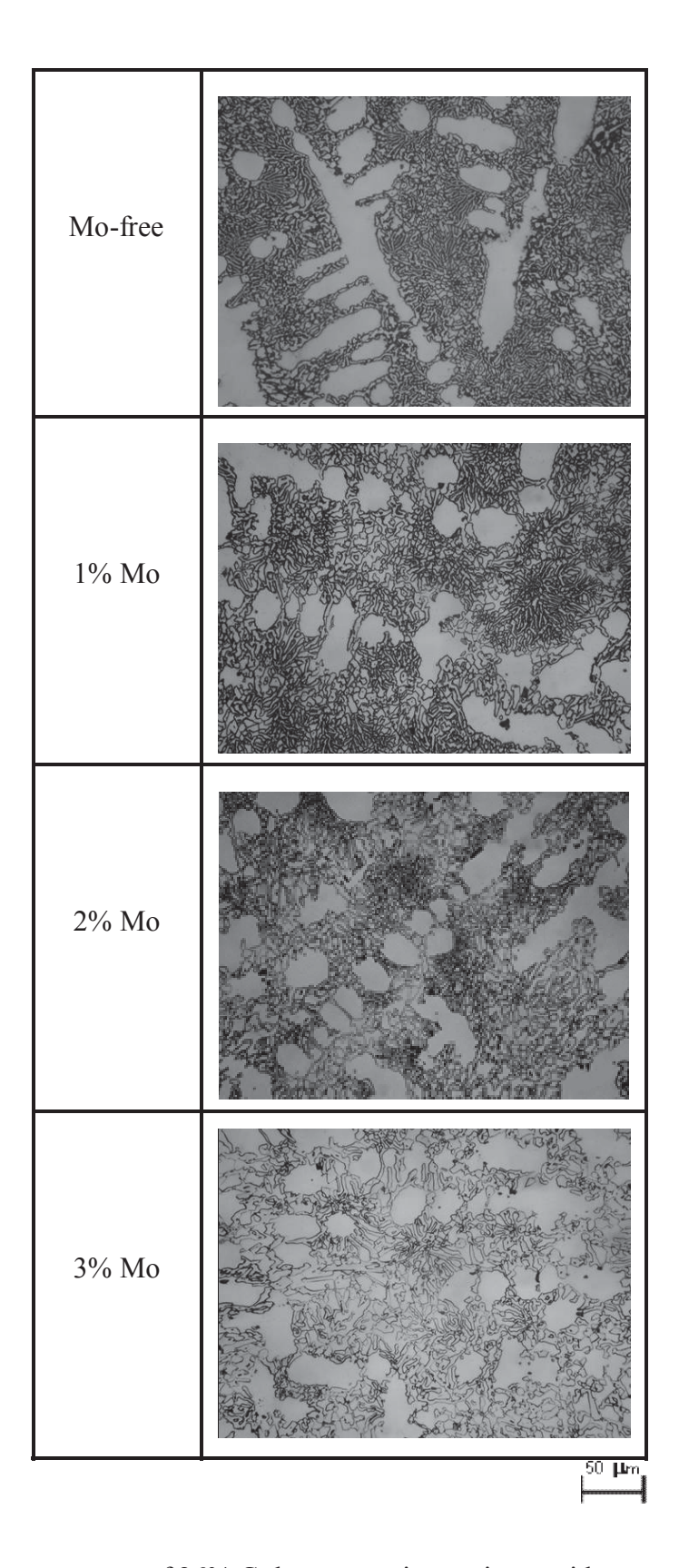


Fig. 2.2 As-cast microstructures of 26% Cr hypoeutectic cast irons without and with Mo. [6]

cast iron without and with Mo. Fully austenitic matrix gives adequate resistance to the abrasive wear under the conditions which allow austenite to work-harden during service. However, too much austenite promotes the spalling wear. Therefore, heat treatment is necessary to control the amount of austenite for higher wear resistance.

As shown in Fig. 2.2, the austenite remains stable in the matrix of each iron. This is because the supersaturation of C and Cr stabilized austenite and depress the Ms temperature below room temperature. G. Laird II [17] reported that Cr retards the transformation from austenite to pearlite. Resultantly, a large amount of austenite remains in the matrix and it leads to low hardness. However, fully austenitic matrix in the as-cast state is desirable under a certain wear circumstances that gives a work-hardened wear surface. A fully austenitic matrix is obtained when [32]

- 1. Ms temperature is below room temperature.
- 2. Sufficient alloying elements are added to avoid the pearlite and bainite transformation.
- 3. Cooling rate after austenitization is high enough not to precipitate secondary carbides in the matrix.

In most cases, the martensitic matrix is preferred to provide high wear resistance. For optimum wear resistance, strength and toughness, an iron with high C and fully martensitic matrix is required. A certain amount of martensite is usually present in the as-cast microstructure, predominantly in localized regions adjacent to the eutectic carbides where the depletion of C and Cr from austenite raised the Ms temperature. If the cooling rate of the casting is slow enough, partial transformation of austenite to pearlite or bainite may take place. [4]

Alloying elements such as Ni, Cu, and Mo are added to high Cr cast irons to increase the hardenability and to prevent austenite from pearlite transformation in the case of heavy section castings. Generally, the alloying element affects the properties of cast iron in two ways. First, it is partially distributed to the austenite during solidification and determines the matrix structure in both the as-cast and heat-treated states. This may improves the properties of matrix. Second, the element remaining in the melt is consumed for the formation of eutectic. In this case, the alloying

element except for the element distributed into eutectic austenite has no longer any effect on the hardenability. [6] Though, the alloying elements such as Mn, Mo, Ni and Cu are normally added to increase the hardenability, the strong carbide formers such as Mo, V and W have been used for special applications when much the higher hardness is required. [33] Laird et al [27] measured the Cr content in the matrix of high Cr cast iron in the as-cast state using electron microprobe analysis. Then, the Cr concentration in the matrix of 3.2%C-28.8%Cr cast iron was only 12.5%. Therefore, a reasonable amount of alloying elements must be added to get sufficient hardenability.

Austenite tends to reject or accept a certain alloying element when it solidifies. The growing austenite will reject C, Cr, Mo, V and Nb which are ferrite forming elements but accept Cu, Ni and Mn which are austenite forming ones. However, Mn dissolves into austenite and carbide. If a large amount of strong carbide forming elements like Mo and V are added into cast iron, they are possible to form special carbides of Mo<sub>2</sub>C and VC which has much higher hardness than chromium carbide (M<sub>7</sub>C<sub>3</sub>). [6] There is a report showing that the special carbides are formed when the content of Mo or V exceeds 2%. [23,24] Mo is added to high Cr cast iron between 0.5-3.5%. However, it should be added more than 1% for effectiveness. [23] Mo acts to suppress the pearlite transformation and improves the hardenability. As shown in Fig. 2.3, the austenitic in the matrix increases when the Mo content is increased. In addition, Mo has little effect on the Ms temperature, while other elements decrease it largely. Mo is relatively expensive, therefore, the decrease of Mo addition was considered. The addition of Cu or Ni instead of Mo is now popular to delay the pearlite transformation and improve the hardenability, because they don't form carbide but dissolve into matrix. [17] Inoculation of Ti refines the eutectic structure. [35]

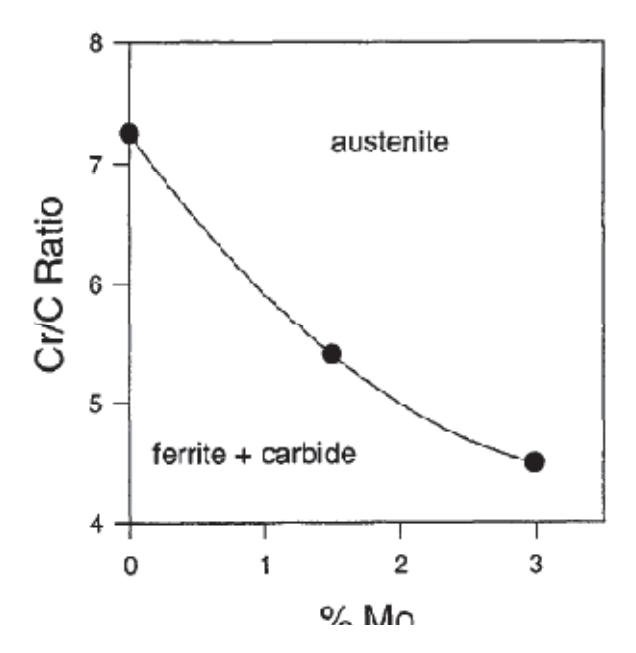


Fig. 2.3 Relationship between Cr/C ratio and Mo content on matrix structure of high chromium cast irons. [16]

The tendency for alloying element to segregate to matrix was observed by Laird. [27] The parameter of segregation ratio (Sr) for each alloying element is introduced using the following equation,

$$S_r = \frac{\% X_{Carbide}}{\% X_{Matrix}}$$

Where %X is the weight percent of each alloy. The results of Sr value using the electron microprobe analysis are summarized in Table 2.2. A high Sr value was obtained in the elements of C and Cr. This suggested that they are strongly segregated to carbides. The Sr values of Cu, Ni and Si are zero. It is indicated that these alloys almost dissolve in the matrix. Dupin [23] investigated the alloy distribution in the austenite dendrite of 17%Cr-2%C cast iron. The results are shown in Fig. 2.4. A slight increase in C and Cr content from the center of dendrite toward the periphery of dendrite can be distinguished. A narrow band near eutectic carbides depleted of C and Cr is due to their diffusion into the eutectic carbides. However, the opposite result is observed by Si.

Table 2.2 Segregation ratios for various alloying element in high chromium cast irons. [27]

Alloy	C	Si	Ni	Cu	Мо	Cr	Mn
15Cr 1Mo 3C	5.4	0.0	0.23	n/a	n/a	4.8	1.3
18Cr 2.2C	6.2	0.0	0.0	0.0	n/a	4.3	1.2
20Cr 2Mo 1Cu 3C	6.1	0.0	0.0	0.0	2.2	4.5	1.0
29Cr 3C	8.8	0.0	0.0	0.0	n/a	4.6	0.8

n/a = not analysed

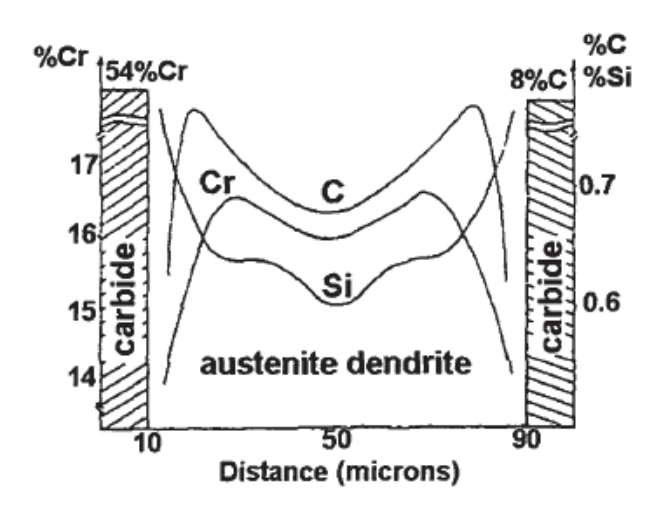


Fig. 2.4 Distribution of alloying elements in austenite dendrite. [23]

### 2.2 Heat Treatment of High Chromium Cast Iron

### 2.2.1 Hardening

Hardening is performed after the destabilization treatment of austenite so that the austenite can transform into martensite. Since the matrix in as-cast high Cr cast iron is austenitic due to supersaturation of C and Cr, a destabilization is necessary to cause the martensite transformation. In the heat treatment process, firstly, the austenite is destabilized by isothermal treatment at high temperature. A usual destabilization temperature for as-cast high Cr cast iron ranges about 950-1100 °C for 1-6 hours depending on alloy content. Powell [27] reported that the secondary carbide precipitation occurred while holding at 1000 °C for 25 minutes. However, at least two hours is need for high Cr cast iron with alloying elements. [1] If the holding time is too long in the case of

heavy section casting, the number of secondary carbides is decreased by Ostwald ripening process.

In the case of high Cr cast iron, the destabilization occurs as follows,

 $\gamma \rightarrow \gamma^* + \text{Secondary carbides } (M_{23}C_6, M_7C_3, \text{ nil or very less } M_3C)$ 

This time,  $\gamma^*$  is destabilized to be lower alloy concentration than that in the as-cast state. The types of secondary carbides could be  $M_{23}C_6$  and/or  $M_7C_3$  depending on chemical composition and holding temperature. For 25% to 30% Cr cast irons, the  $M_{23}C_6$  carbides are mainly formed, whereas  $M_7C_3$  and  $M_{23}C_6$  carbides form in 15% to 20% Cr cast irons. [37] It has been reported that the precipitation of secondary carbide produces in two stages, the  $M_{23}C_6$  carbide precipitates first and then transform to  $M_7C_3$  when it is held for a long time. [26,27,37] As a result of the secondary carbides precipitation, the C and Cr content in austenite is reduced and the Ms temperature is raised. The high Cr cast irons are usually hardened by fan air cooling after destabilization treatment to room temperature. An important requirement is that the cast iron must show sufficient hardenability to avoid the pearlite transformation during cooling.

Fig. 2.5 shows the typical as-hardened microstructure of 16% Cr cast iron with 3% Mo. In the matrix, the secondary carbides, martensite and small amount of retained austenite can be observed. [7] The M<sub>2</sub>C carbides are clearly detected in the SEM micrographs of 3% Mo specimen. [6] Powell [26] reported that the secondary carbides which precipitated in the matrix are mostly M<sub>23</sub>C<sub>6</sub> carbides co-existing with small amount of M<sub>7</sub>C<sub>3</sub> carbides.

The destabilization temperature has a major effect on the amount of retained austenite and final hardness. Maratray and Poulalion [38] showed that the main factors controlling the amount of retained austenite are chemical composition, holding temperature and cooling rate. For the high Cr cast iron, the maximum hardness is achieved at the destabilization temperature between 950-1050 °C as shown in Fig. 2.6. The maximum hardness has been obtained at about 20%  $V_{\gamma}$ . [3,38] S. Inthiech [3] showed that the proportion of retained austenite after destabilization at 1050 °C was greater than that at 1000 °C destabilization.

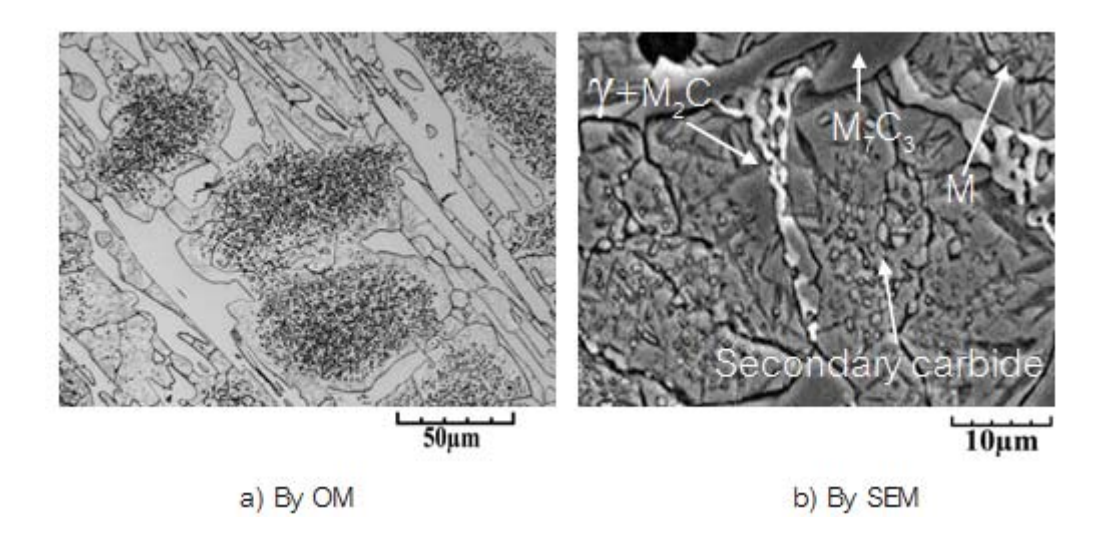


Fig. 2.5 Microphotographs of as-hardened specimens with Mo by OM and SEM. [7]

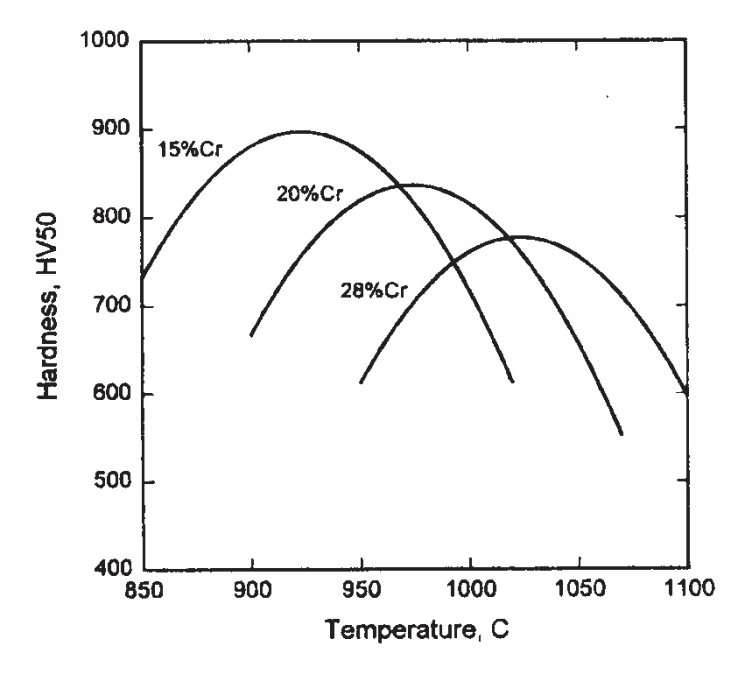


Fig. 2.6 Effect of destabilization temperature on the maximum hardness of high chromium cast irons. [33]

Maratray [16] suggested that an optimal destabilization temperature for maximum hardness in air hardening arises from as follows,

- 1. At high temperature, the solubility of carbon in austenite is high. The high carbon content depresses the Ms temperature producing the large amount of retained austenite after air cooling.
- 2. At low temperature, the carbide precipitation reduces the carbon content in austenite. The low carbon martensite forms during cooling and the relative low hardness is obtained.

From Fig. 2.7, the maximum hardness is obtained at about 1025  $^{\circ}$ C. The amount of retained austenite ( $V_{\nu}$ ) increases with increasing the austenitizing temperature.

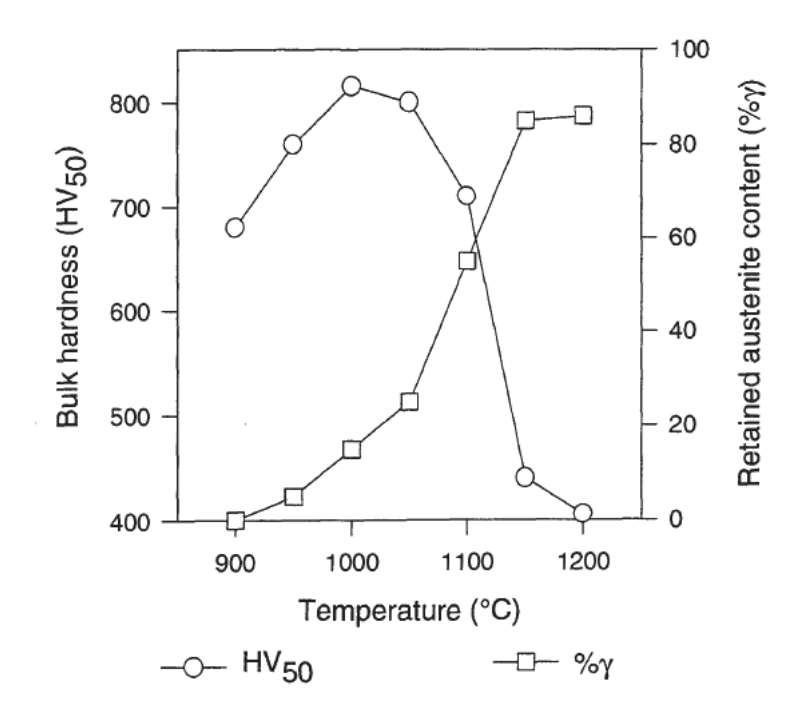


Fig. 2.7 Effect of destabilization temperature on hardness and volume fraction of retained austenite. [16]

The addition of alloying element also affects the amount of retained austenite due to the stabilization of austenite. The carbon content in the matrix has greatest influence on the Ms temperature. Increasing the carbon content can increase the hardenability and the hardness. However, it also increases the amount of retained austenite. There is a report concerning Ms temperature or hardenability by S.Inthidech. [6] The hardenability increases with an increase in Cr/C value and with an addition of Ni, Cu and Mo. The volume fraction of retained austenite in the as-hardened state of 16% Cr cast iron was increased by Ni, Cu and Mo additions but decreased by V addition as shown in Fig. 2.8. Cu and Ni almost dissolve in the austenite and lower the Ms temperature. Mo and V, strong carbide forming elements, prefer to dissolve in the eutectic carbides during solidification. Only the rest of elements consumed in carbide formation dissolves in the austenite and affects the Ms temperature.

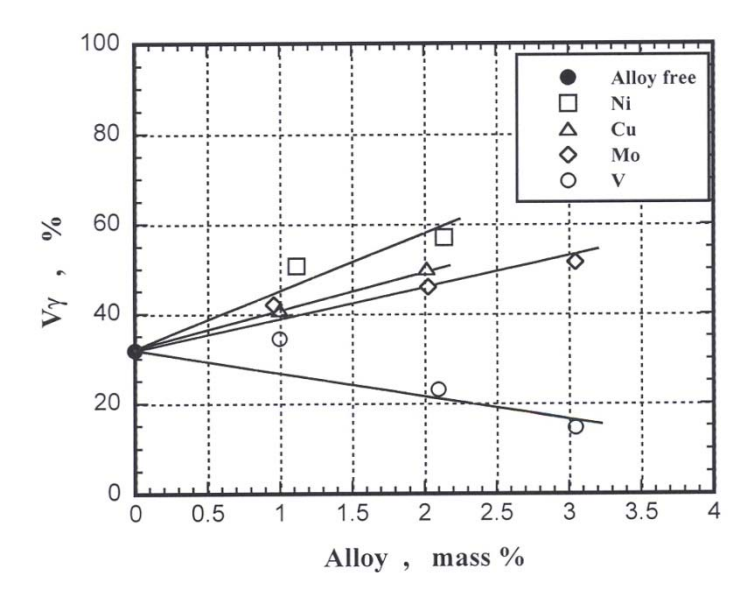


Fig. 2.8 Effects of alloying elements on the volume fraction of retained austenite ( $V_{\gamma}$ ) in the ashardened state of 16% Cr cast iron. [6]

### 2.2.2 Tempering

Tempering is the final heat treatment stage to produce the desired properties of materials. Tempering is always recommended after hardening. The main purpose is to decompose martensite and retained austenite to control the hardness, of course, the residual stress caused by hardening should be reduced by tempering. The main reaction is to destabilize the retained austenite to bring about the martensite transformation on cooling. Sudsakorn [6] reported that the secondary hardening in tempering of high Cr cast iron is considered to occur by the following reactions;

- Decomposition of as-hardened martensite, that is to say, precipitation of secondary carbides from martensite. Finally, this ends with "carbide reaction".
- II. Decomposition of retained austenite in the as-hardened state, in other words, precipitation of carbides from retained austenite.
- III. Transformation of retained austenite after precipitation of secondary carbides into martensite during cooling.

Each reaction acts the part of an increase in hardness. However, the increasing degree of hardness could be greater in the reactions (I) and (III), but the effect of reaction (II) is probably small. Martensite formation after tempering is attributed to the precipitation of secondary carbides in the retained austenite during tempering. Because of the reduction of C and Cr contents in the retained austenite, Ms temperature increases and martensite transformation appears on cooling to room temperature.

The tempering temperature and holding time must be carefully chosen to avoid overtempering that leads to a decrease in hardness and strength of the matrix. Tempering temperature between 200 and 450 °C is too low to make the retained austenite transform, and temperature in the range of 500 to 600 °C is appreciated. [1] Maratray [38] reported that in the range of tempering temperature from 480 °C (753K) to 650 °C (923 K), M<sub>23</sub>C<sub>6</sub> carbide is more stable than M<sub>7</sub>C<sub>3</sub> carbide and so M<sub>23</sub>C<sub>6</sub> carbide could precipitate from retained austenite at the temperature over 480 °C (753 K). [34] Sare and Arnold [4] said that tempering treatment of 27% Cr cast iron at 500 °C (773 K) reduced the retained austenite below 10 vol%. In 15% Cr cast irons with C

content less than 1.5%, the toughness is increased with increasing the tempering temperature. [1] For over 1.5% C, the toughness is not controlled by varying the tempering temperature but controlled by the amount of eutectic carbides.

The effect of alloying elements on the hardness and  $V_{\gamma}$  during tempering was reported by S. Inthidech. [3] It was found that the hardness curve showed the secondary hardening. The degree of secondary hardening was greatest in Ni bearing specimen followed by Cu, Mo and V, respectively and the cast iron with Mo showed the highest hardness. Fig. 2.9 shows the tempering behavior of 26% Cr cast irons with and without Mo. The tempered hardness curves show evident secondary hardening due to the precipitation of secondary carbides and the transformation of austenite to martensite. The degree of secondary hardening increases with increasing of Mo content. The amount of retained austenite decreases when the tempering temperature rises. The maximum hardness is obtained at the tempering temperature 500-525 °C. The temperature over this temperature, the hardness is decreased due to the coarsening of secondary carbides. It is also found that the cast irons with large amount of retained austenite give a large degree of secondary hardening and the hardness is higher than that in its as-hardened state.

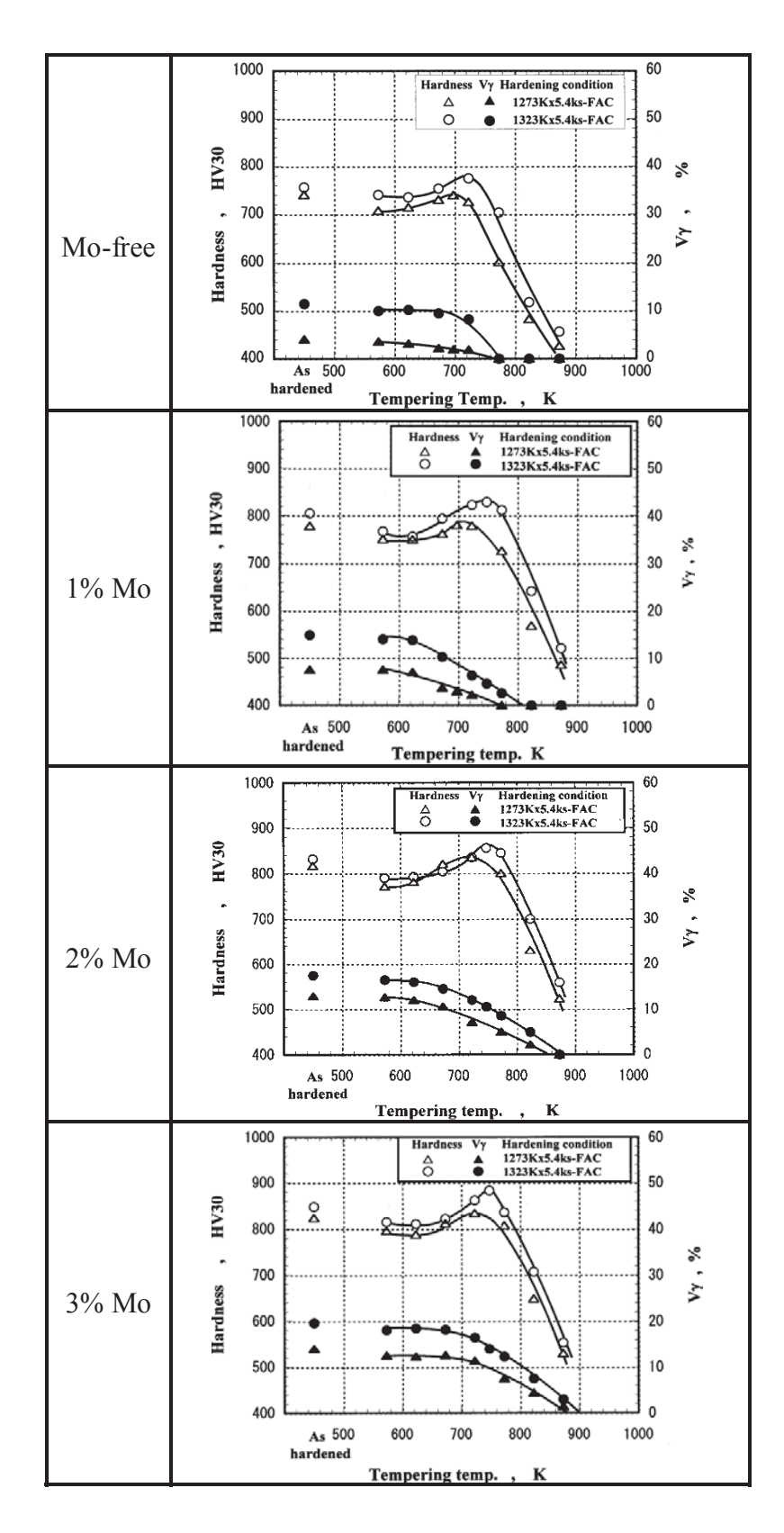


Fig. 2.9 Relationship between hardness, volume fraction of retained austenite  $(V_{\gamma})$  and tempering temperature of 26% Cr cast irons with and without Mo. [3]

#### 2.3 Abrasive Wear

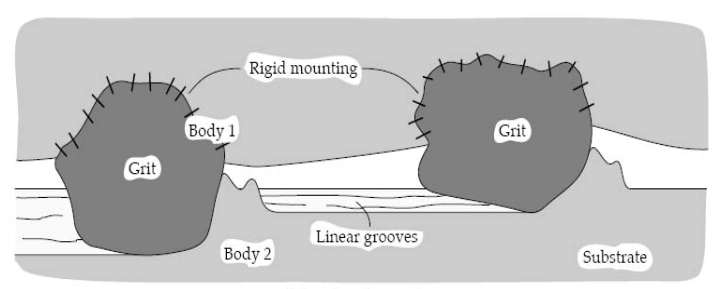
Wear can be defined as the removal of materials from the surface of body moving in contact with another material or counterpart. The rate of wear depends on several factors such as surface microstructure, type of materials, relative movement, chemical action, service circumstance like moisture and temperature. Abrasive wear occurs due to the action of abrasive particles or fragment on the surface of component. It occurs usually in the various kinds of machines which are used for digging, crushing, milling or pulverizing and rolling in the fields of mining, iron and steel, electric power plant and cement industries. Abrasive wear can be described as two basic types, Two-body and Three-body types as shown in Fig. 2.10. Two-body type abrasive wear occurs when two working surfaces are contacted to grind those angular materials. The stress in this wear process is high enough to crush the particles. On the other hands, three-body type abrasive wear occurs in the portion where freely moving particles exist between the surfaces of components. The stress is not high enough to cause crushing of the abrasive particle. This type of wear takes place in the ball mills and tube mills in the cement, steel and mining industries.

There are many mechanisms for abrasive wear. Fig. 2.11 shows the ideal cross section of wear grove. Area A1 is a size of wear groove, while A2 is a size of materials welled plastically to the side of groove. The wear rate (Rw) is calculated using the following relation, [40]

$$Rw = \frac{\left(A_1 - A_2\right)}{A_1}$$

The mechanism of wear can be summarized as follows,

- 1. Ploughing: the material displaces either side of the wear groove as shown in Fig. 2.12 (a). There is no materials remove directly in the wear process. So, the area of A2 equals to area of A1.
- 2. Cutting: the material is removed as debris of microchip without displacement. Volume of wear loss equals to that of material removal as shown in Fig. 2.12 (b).



Two-body mode

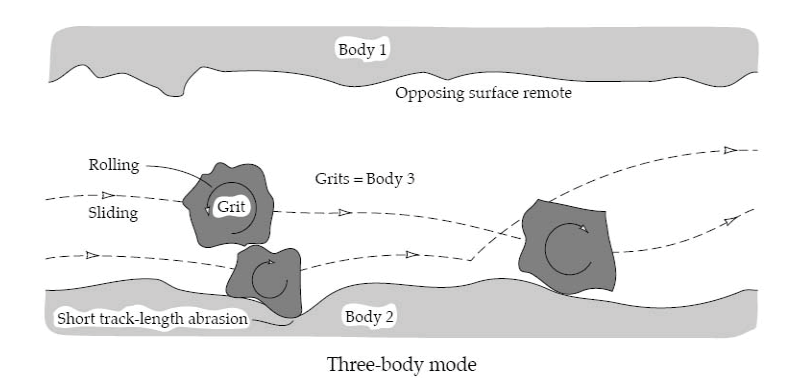


Fig. 2.10 Main type of wear. [39]

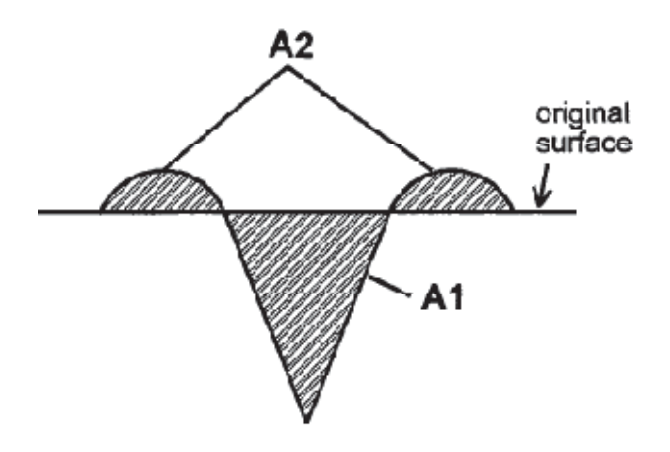


Fig. 2.11 Ideal cross section of wear groove. [40]

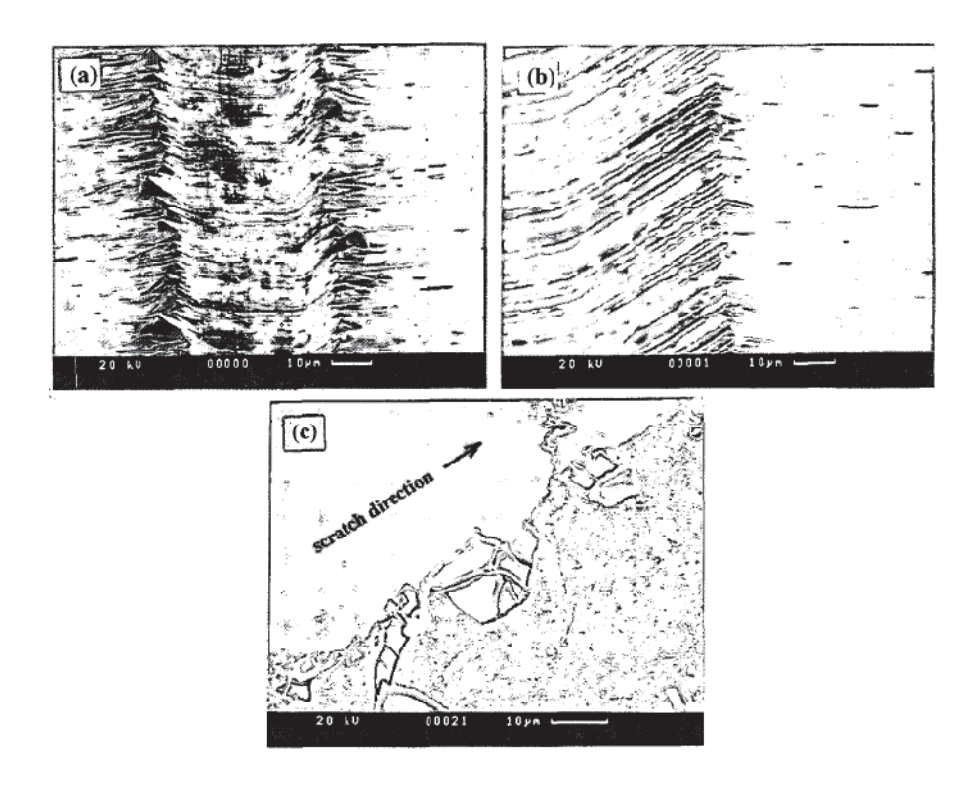


Fig. 2.12 Example of ploughing, cutting and fragmentation in the worn surface using scratch test. [41]

3. Fragmentation: cracks form the surrounding and at the surface of wear groove as shown in Fig. 2.12 (c). This crack leads to formation of spall and removal of material. The volume of wear loss may exceed the volume wear groove.

It has been suggested that the parallel movement between abrasive material and worn surface produces the ploughing and cutting, while relative vertical motion leads to fragmentation. The plastic deformation behavior of materials also determines the wear mechanism

There are several methods to investigate the wear resistance of materials, and they are summarized in Fig. 2.13. For each test, standard condition of load, dimension of specimen, wear distance are used and the mass loss due to abrasion wear is measured. It is well known that there are many factors to determine the wear resistance. The microstructure plays very important

role. In high Cr cast iron, the microstructure varies depending on size of casting or solidification rate, alloy addition and heat treatment conditions.

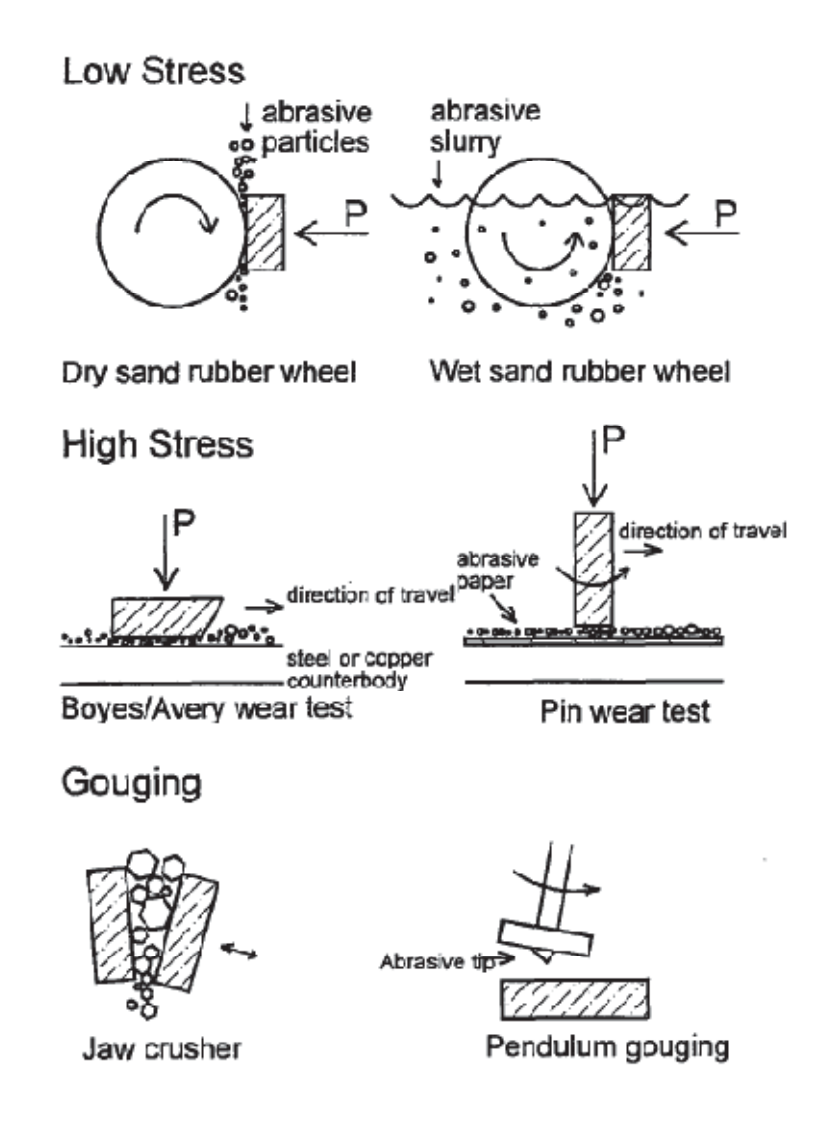


Fig. 2.13 Schematic drawings of abrasive wear tests. [20]

In general, wear resistance is related to the type and morphology of carbides and the matrix structure. [17-19,42] The effects of carbide type and its hardness can be apparently estimated comparing the hardness of carbides with that of the abrasive materials. It is well known that high Cr cast iron contains the eutectic carbides of M<sub>7</sub>C<sub>3</sub> type which has a higher hardness than that of the abrasive materials like quartz and garnet. This cast iron shows the excellent wear resistance against these minerals. The addition of Mo, V or Nb to high Cr cast iron can improve the abrasion wear resistance due to the increase in the hardness. It was reported that the rate of wear increased with an increase in the hardness and with a decrease in the size of abrasive

particles. [1,40,43] Table 2.3 shows the relative hardness of abrasive materials and carbides in high Cr cast iron. The hardness of M<sub>7</sub>C<sub>3</sub> carbide is higher than those of quartz and garnet which commonly encountered in service of mining industry. However, the hardness of M<sub>7</sub>C<sub>3</sub> carbide is lower than the hardness of silicon carbide and alumina. From these points of view, it is considered that addition of V which forms very hard vanadium carbide provides the excellent wear resistance.

Table 2.3 Hardness of abrasive materials related to hardness of microstructure of high Cr cast iron. [20]

Abrasive Material	Har	rdness	Microstructural Constituen	
	Kncop	HV		
	2660	2800	Vanadium carbide	
Silicon carbide	2585	2500-2600		
Corundum (Al <sub>2</sub> O <sub>3</sub> )	2020	1800-2000		
	1735	1200-1800	M <sub>7</sub> C <sub>3</sub> -type carbide	
		1060-1240	M <sub>5</sub> C-type carbide	
Garnet	1360			
Quartz (silica)	840	900-1280		
		770-800	High-carbon martensite	
		350-400	Austenite	

Under high stress abrasion, the effect of volume fraction of carbide (Vc) on wear resistance depends on the hardness of abrasive materials. If softer abrasive material than carbide hardness is used, the wear resistance increases with increasing Vc. However, when the harder abrasive material is used, an increase in Vc do not show the significant effect on wear resistance. As shown in Fig. 2.14, it is found that the wear loss increases with an increase in Vc when SiC is used. This is because the harder abrasive material could indent into carbides leading to spalling and pitting. The inverse relation is obtained when garnet is used as abrasive material. [40]

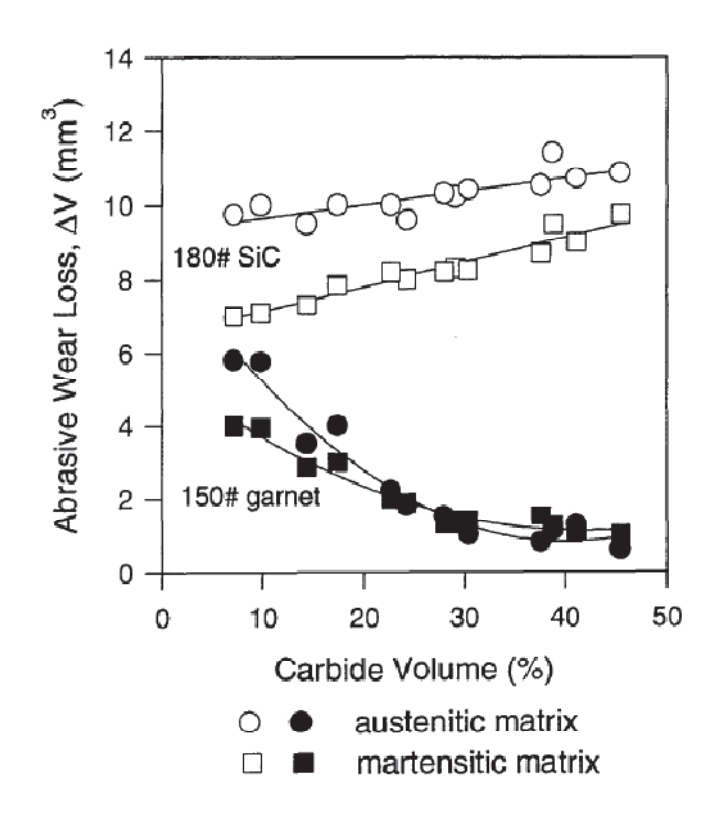


Fig. 2.14 Effect of volume fraction of carbide on abrasive wear loss. [40]

Dogan et al. [14] reported that the carbides aligned appareled to the wear surface give the best wear resistance by a pin on disk abrasion test. He also studied the abrasion wear resistance of as-cast 15% and 26% Cr cast irons. As shown in Fig. 2.15, the wear rate decreased with increasing the volume fraction of carbide when matrix is the same. It can be also concluded that the abrasive wear resistance of as-cast 26% Cr cast iron, which has more austenite in the matrix and high volume fraction of carbide, is better than that of as-cast 15% Cr cast iron with bainitic and pearlitic matrix and with lower volume fraction of carbide. In the same way, wear resistance increases with an increase in the macro-hardness as shown in Fig. 2.16. It has been reported that the increasing of the carbide volume fraction resulted in the decrease of wear rate to the soft abrasives such as hematite and phosphate rock, because of protection of the matrix by carbides in eutectic microstructure. [43]

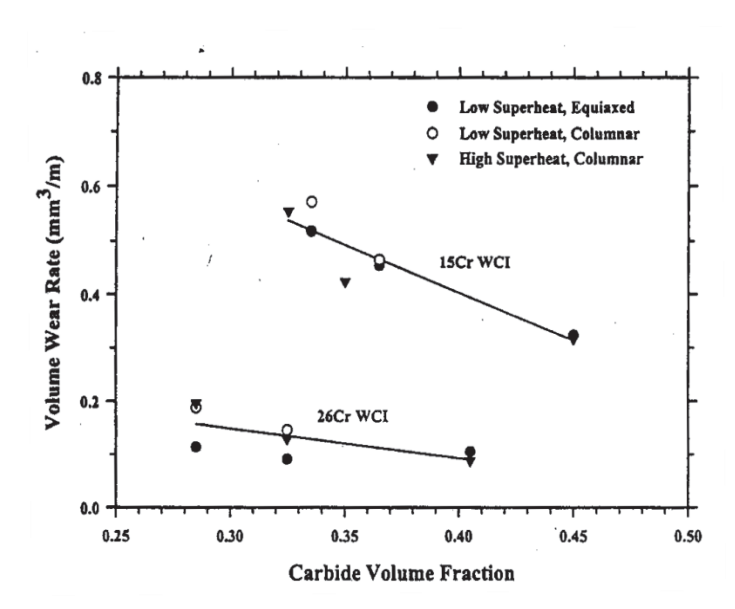


Fig. 2.15 Relationship between wear rate and volume fraction of carbide of high chromium cast irons. [14]

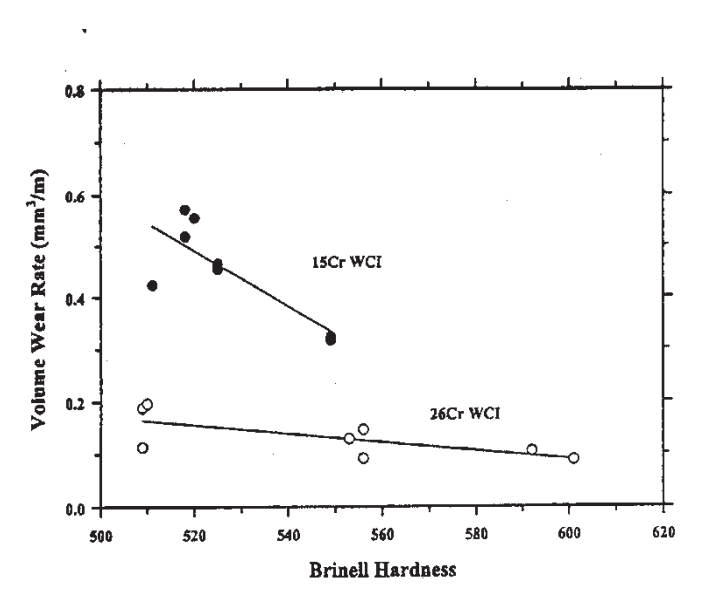


Fig. 2.16 Relationship between wear rate and hardness of high chromium cast irons. [14]

As described previously, the volume fraction of carbide has shown the strong influence on the wear resistance. The 30% volume fraction of carbide provides the best abrasion wear resistance in the heat treated white cast iron. [35] Although wear resistance is generally increased with increasing the volume fraction of carbides, the wear behavior varies depending on the wear system or wear mechanism under the service condition.

It has been said that the higher the matrix hardness, the greater is the wear resistance. The matrix influences on the degree to protect the carbide. If the matrix is not protected and preferentially removed, the carbide may fracture and spall. It was reported that the pearlitic matrix showed the poor wear resistance. [44] The austenitic matrix is preferred under the harder abrasive material, while the martensitic matrix shows the best wear resistance with softer abrasive material. [15] This occurs according to the work hardening effect.

The heat-treated high Cr cast irons with martensitic matrix have a higher wear resistance but sometimes poorer toughness than austenitic and pearlitic matrix. [1,4,9,10,14,18,19,29,31,34-36] By Dogan et al, [15] the pearlitic matrix has extremely poor wear resistance compared with the matrix mixed with austenite and martensite. An austenitic matrix leads to better abrasion wear resistance compared with the pearlitic matrix because of work-hardening ability of austenite on the worn surface. Sare et al [4] reported that the volume fraction of retained austenite which gives the highest wear resistance lies in 40-50% for gouging abrasion as shown in Fig. 2.17. Sare et al [34] also studied on high stress abrasion pin test and reported that the largest wear resistance is obtained in the as-hardened state containing volume fraction of retained austenite more than 20%. As shown in Fig. 2.18, the results of a pin-on-disk test result by Zum Gahr [40], showed that an increase in retained austenite leads to greater wear rate with garnet as abrasive. When SiC is used, by contrast, the wear loss decreases with increasing of retained austenite. It could be due to the stain-induced-martensite and high toughness of austenite.

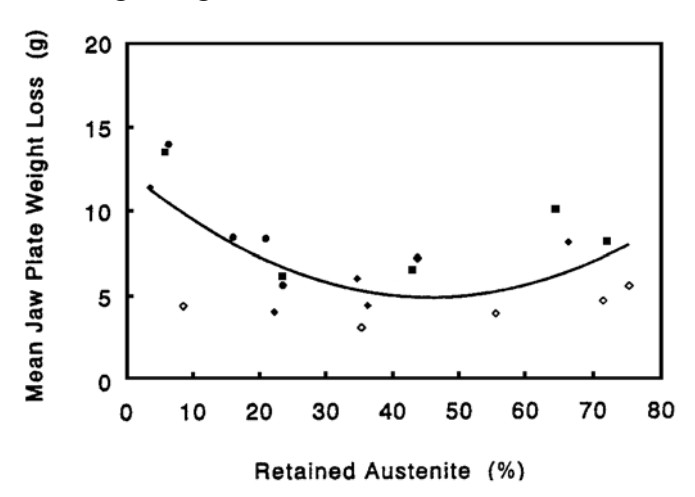


Fig. 2.17 Relationship between mean weight loss (g) and volume fraction of retained austenite by jaw plate test. [4]

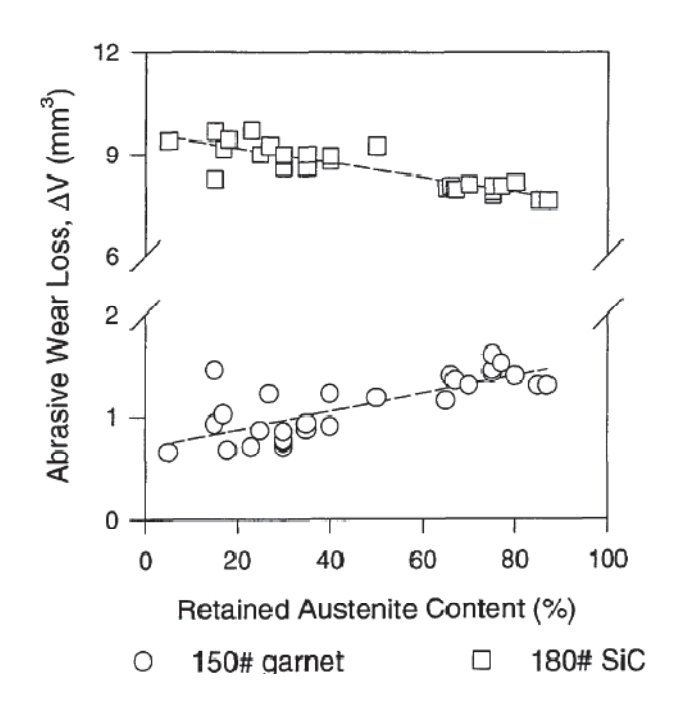


Fig. 2.18 Effect of retained austenite content on abrasive wear loss of 2.9% C-19% Cr-2.35% Mo cast iron. [40]

It was found that the wear resistance was related to carbon content. As shown in Fig. 2.19, the wear loss decreased as the C content increased to 3% at about eutectic composition of 30% Cr cast iron, and then became steady. It has been suggested that as C content increases, the volume fraction of carbides increased high enough to protect the matrix. In fact, the toughness will decrease when the C content increases over eutectic composition, but the wear resistance is balanced due to the precipitation of brittle hyper-eutectic carbides.

Phasit et al [8] used Suga abrasion wear tester and Rubber Wheel abrasion wear tester to investigate the two-body type and three-body type abrasion wear behaviors in hypoeutectic 16% Cr cast iron containing molybdenum. It was found that the wear rate was decreased with an increase in Mo content because Mo improves the hardenability in the heat treatment and promotes the precipitation of Mo carbides with high hardness. Sudsakorn et al [7] studied the abrasive wear of hypoeutectic 16% Cr cast iron containing Mo. The data are not so scattered as Sare's results [4] as shown in Fig. 2.20, and the smallest wear rate was obtained at 20 to 25% V<sub>γ</sub>. Fig. 2.21 shows the effect of hardness and Mo content on the wear rate. It is clear from this results that the wear rate decreased proportionally as the macro-hardness is increased regardless of Mo contents of cast irons. When the wear rate is connected to the Mo content, as shown in Fig. 2.22, however the

wear rate trends to decrease totally with increasing the Mo content. It can be suggested that an increase in Mo content up to 3% improves the wear resistance of hypoeutectic 16% Cr cast iron. Using a ball mill test, the effects of carbide volume fraction and matrix structure on the abrasive wear resistance of high Cr cast iron balls tested were investigated by Albertin and Sinatora.[43] As shown in Fig. 2.23, it was found that the martensitic matrix showed the highest wear resistance against three kinds of abrasives of phosphate rock, hematite and quartz. When the ratio of hardness of the abrasive and matrix (H<sub>a</sub>/H<sub>m</sub>) is taken into consideration, it was found that the wear resistance decreased as the H<sub>a</sub>/H<sub>m</sub> increased as shown in Fig. 2.24. [43]

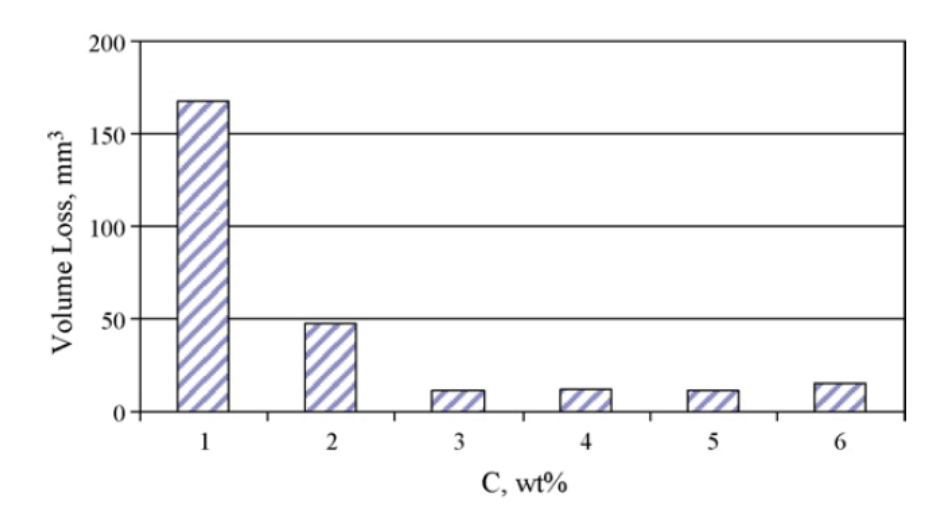


Fig. 2.19 Relationship between wear loss and C content of 30% Cr cast iron. [29]

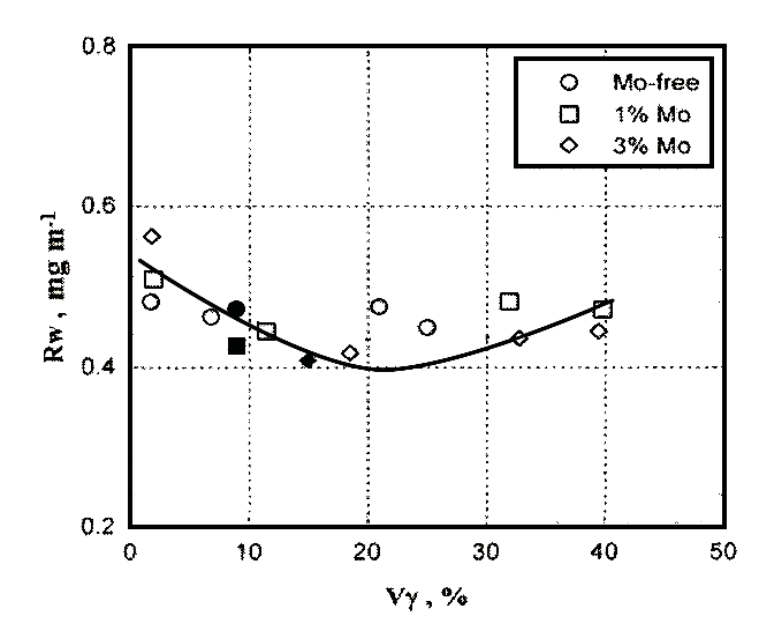


Fig. 2.20 Relation between wear rate (Rw) and volume fraction of retained austenite ( $V_{\gamma}$ ) of hypoeutectic 16% Cr cast iron. [7]

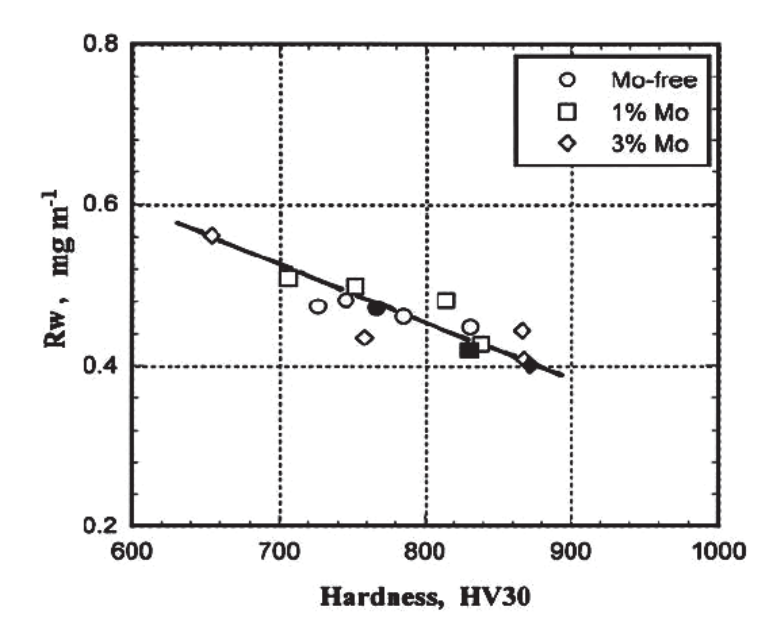


Fig. 2.21 Effect of Mo content on relationship between the wear rate (Rw) and macro-hardness of hypoeutectic 16% Cr cast iron. [7]

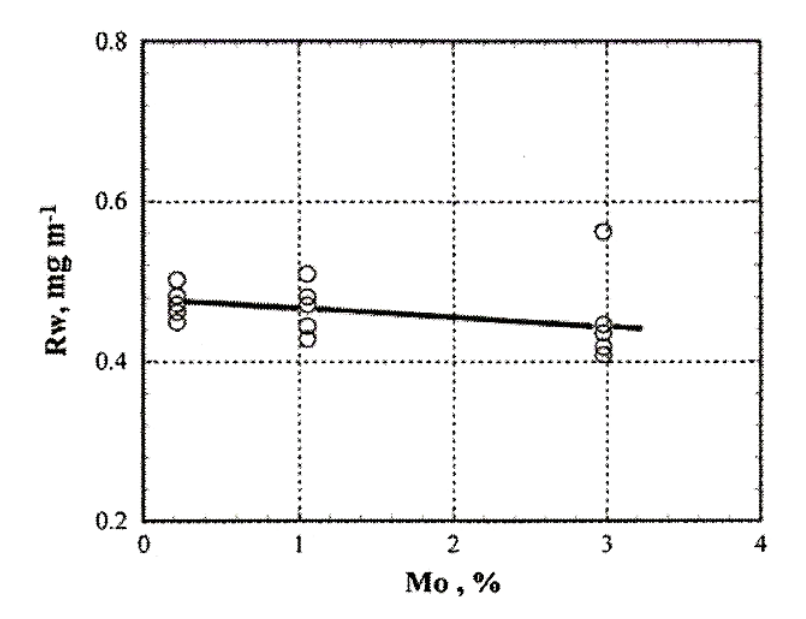


Fig. 2.22 Effect of Mo content on the wear rate (Rw) of hypoeutectic 16% Cr cast iron. [7]

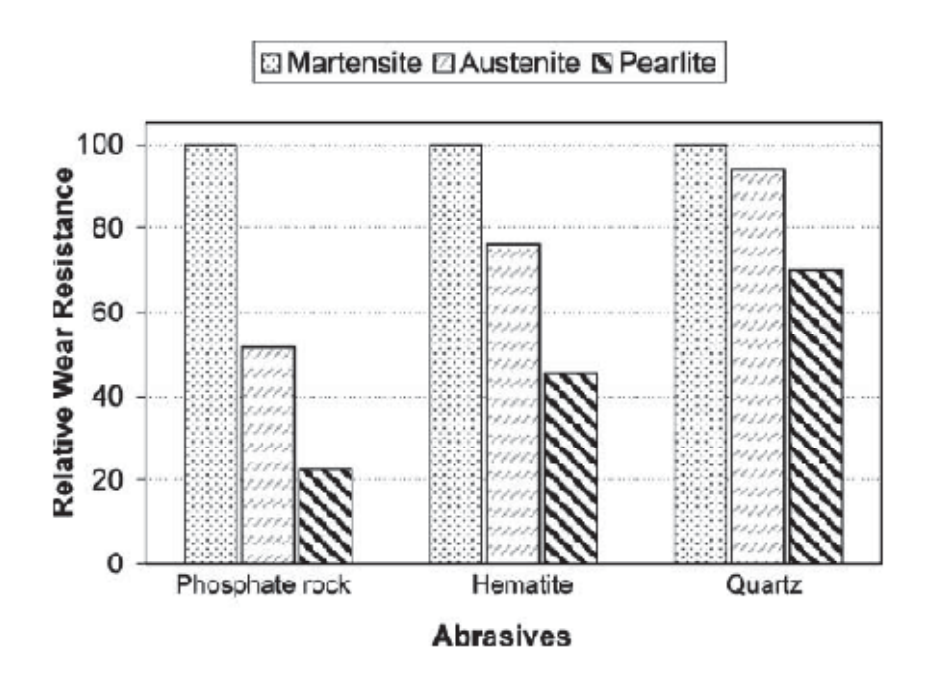


Fig. 2.23 Effect of matrix structure on relative wear resistance of high Cr cast irons. Ball mill test. [43]

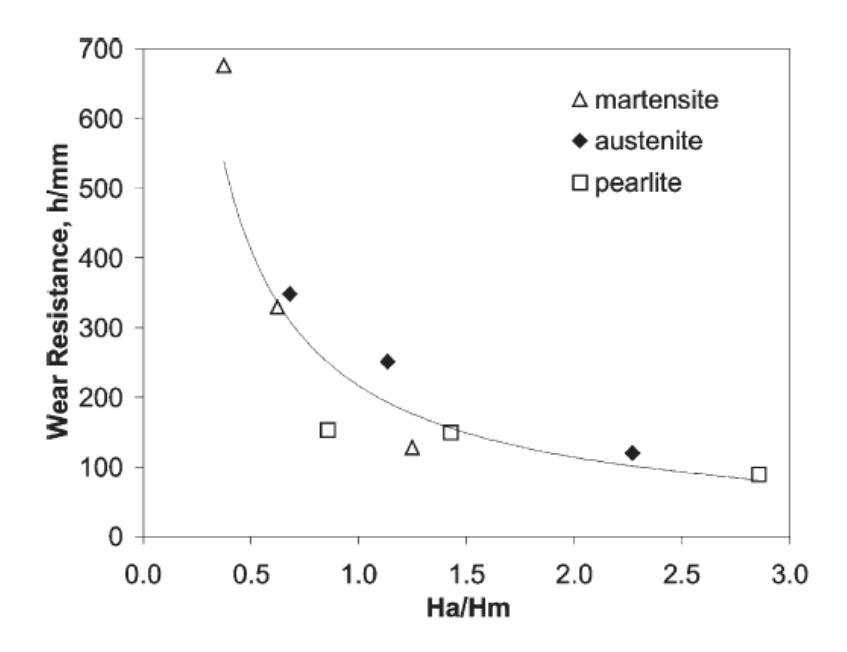


Fig. 2.24 Effect of ratio of abrasive hardness and matrix hardness (Ha/Hm) on the wear resistance. [36]

## Chapter 3

# **Experimental Procedure**

# 3.1 Preparation of Specimens

The schematic drawings of process to make ingot and test pieces are shown in Fig.3.1. The charge calculations are carried out for the target chemical compositions of hypoeutectic 16% Cr cast irons. As raw materials, mild steel scrap, pig iron, ferro-alloys, pure metals are used. The total weight of 30 kg of charge materials is melted down in a high frequency induction furnace with alumina (Al<sub>2</sub>O<sub>3</sub>) lining and superheated up to 1853 K (1580 °C). After holding, the melt is poured at 1773-1793 K (1500-1520 °C) into the preheated CO<sub>2</sub> mold in Y-block shape of which cavity size of specimen is 50x50x200 mm. After pouring, the melt is immediately covered with dry exothermic powder to hold the temperature of riser (Fig.3.1(a)). The chemical compositions of the test specimens are summarized in Table 3.1.

The riser part was cut off from Y-block ingot and the substantial block is supplied for annealing to remove the casting stress and micro-segregation produced during solidification. The substantial block is coated with an anti-oxidation solution to prevent the block from oxidation and decarburization. The block in an electric furnace was heated up from room temperature to 1173 K (900°C) with a heating rate of 0.1 K/s and held for 18 ks (5 hours) and follow by cooling in the furnace to the room temperature. In order to make test pieces for abrasion wear test, the block was sliced into pieces with 7 mm in thickness using a wire-cut machine called EDM (Electric Discharge Machine). The process of making test pieces is shown in Fig. 3.1(c).

**Table 3.1** Chemical composition of specimens.

Specimen	Element (wt%)				
1	С	Cr	Si	Mn	Mo
No.1	2.66	26.08	0.47	0.55	0.18
No.2	2.64	26.12	0.50	0.56	1.02
No.3	2.63	25.92	0.44	0.45	1.97
No.4	2.71	25.98	0.47	0.53	2.96

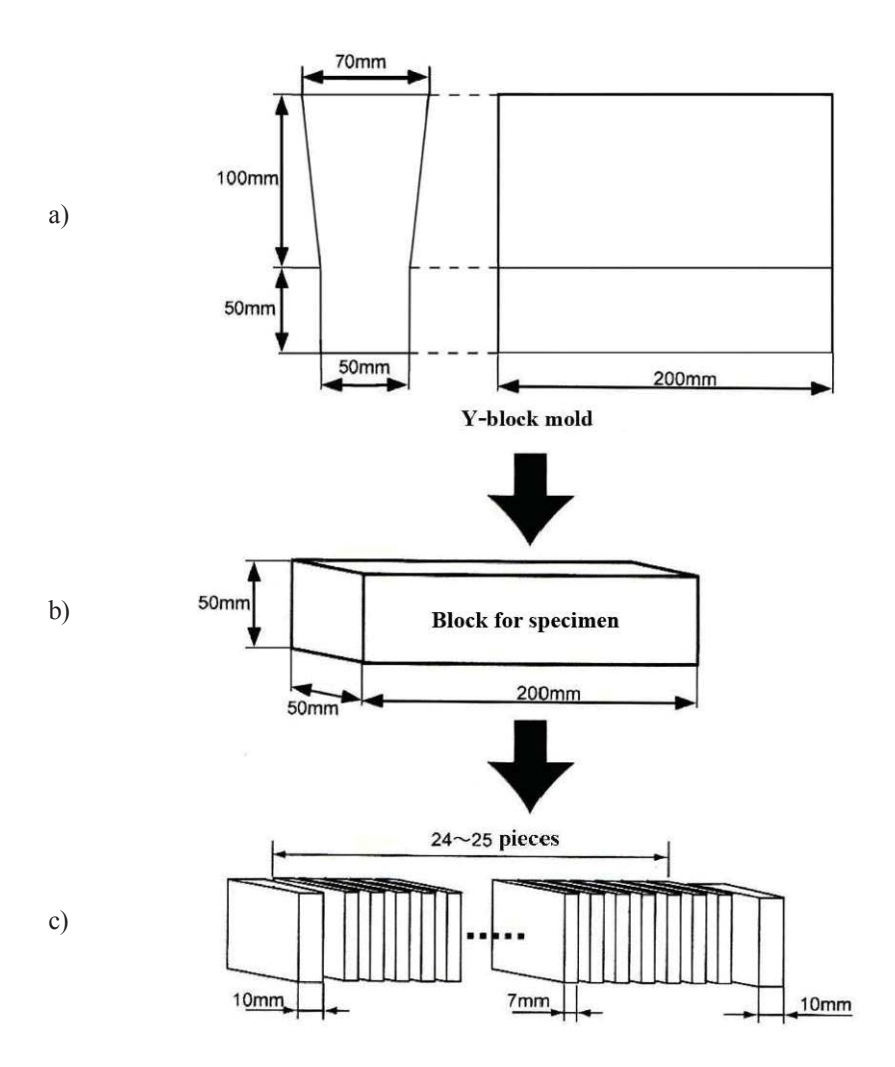


Fig. 3.1 Process of making test pieces.

## 3.2 Heat Treatment Procedures

The conditions of heat treatment are listed in Table 3.2. The sliced test pieces were also coated by the anti-oxidation solution and dried at 473K (200°C) in an electric furnace. They were heated up to 1323 K (1050 °C) for austenitization. After holding for 5.4 ks (1.5 hours), the test pieces are hardened by fan air cooling. The hardened test pieces are tempered in a furnace at 3 levels of temperatures from 673 to 873 K. The tempering temperatures were determined according to the reference [3] and they are shown in Table 3.3. After tempering, the test pieces are cooled to the room temperature by fan air cooling.

Table 3.2 Heat treatment condition.

Heat Treatment Process	Annealing	Hardening	Tempering
Temperature (K)	1173	1323	3 levels between
Holding Time (ks)	18.0	5.4	7.2
Cooling Condition	Furnace Cooling	Fan Air Cooling	Fan Air Cooling

Table 3.3 Tempering temperature.[3]

G .	Tempering temperature (K)			
Specimens	L-H <sub>Tmax</sub>	$H_{Tmax}$	H-H <sub>Tmax</sub>	
26%Cr Mo-free	673	723	773	
26%Cr-1%Mo	673	748	800	
26%Cr-2%Mo	673	748	800	
26%Cr-3%Mo	673	748	823	

### 3.3 Observation of Microstructure

## 3.3.1 Optical Microscopy

To observe the microstructure by means of an optical microscope (OM), the specimen is polished using emery papers in the order of #180, 320, 400 and 600 and finished by a buff cloth with extremely fine alumina powder of  $0.3~\mu m$  in diameter. The microstructure is revealed using the etchants shown in Table 3.4.

Type Etchant Etching method Attack Pieric acid 1 g + HCl 5 Carbide and Immersion at Α cc + Ethanol 100 cc room temperature matrix HNO<sub>3</sub> 5 cc + Ethanol Immersion at В Matrix 95 cc room temperature

Table 3.4 List of etchants.

## 3.3.2 Scanning Electron Microscopy

For more discussions, the microstructure involving secondarily precipitated carbides are observed in detail using a Scanning Electron Microscope (SEM). A polished specimen is lightly etched using the etchant A to reveal the microstructure. The microphotographs mainly focusing on the carbide morphology in matrix are taken with high magnification.

## 3.4 Hardness Measurement

Macro-hardness of test pieces is measured by means of Vickers hardness tester applying the load of 297 N (30 kgf) and micro-hardness by Micro-Vickers hardness tester applying the load of 1 N (100 gf). In each test pieces, the hardness is measured five at different places and their average values are adopted.

## 3.5 Measurement of Volume Fraction of Austenite $(V_{\gamma})$

## 3.5.1 Theory for Measurement of Austenite by X-ray Diffraction Method

Quantitative measurement of austenite in matrix is not so easy because the bulk test specimen with strong orientation of dendrite must be used. In the methods to measure the volume fraction of austenite, X-ray diffraction method is convenient when the texture is cancelled as if the powder sample is used.

The basic equation of diffraction intensity of a phase is expressed as

$$I_{hkl} = K(FF^*)(LPF)me^{-2M}A(\theta)V_i/v_i^2$$
(3.1)

where, K =proportional constant

FF\* = structure factor of the unit cell of the interest phase, equal to  $4f^2$  and  $16f^2$  for diffraction lines of  $\alpha$ (martensite/ferrite) and  $\gamma$  (austenite), respectively, where f is the atomic-scattering factor of the species of atom which make up the unit cell: f relates to  $(\sin \theta)/\lambda$ 

LPF = Lorenz Polarization Factor,  $(1+\cos^2 2\theta)/\sin^2 \theta \cos \theta$ 

m = multiplicity factor, the number of {hkl} planes in a unit cell

e<sup>-2M</sup> = Debye –Waller temperature factor where

 $M = (B\sin^2\theta) / \lambda^2 : B \text{ is a material constant}$ 

 $A(\theta)$  = absorption factor, independent of  $\theta$  if sample is flat

 $V_i$  = volume fraction of the phase

 $v_i$  = volume of unit cell

Let, 
$$K' = K \times A(\theta)$$
 (3.2)

and 
$$R_{hkl} = [FF*(LPF)me^{-2M}]/v_i^2$$
 (3.3)

Here, Debye-Waller temperature factor is negligible. Substitutes K' and  $R_{hkl}$  in the equation (3.1) to be equation (3.4),

$$I_{hkl} = K'R_{hkl}V_i \tag{3.4}$$

When several peaks in the diffraction pattern participate in the calculation, the above equation is shown by the next equation (3.5),

$$\Sigma I_{hkl} = K'(\Sigma R_{hkl})(V_i) \tag{3.5}$$

Therefore, peaks of ferrite and/or martensite ( $\alpha$ ) and peaks of austenite ( $\gamma$ ) are respectively shown as

$$\Sigma I_{\alpha} = K'(\Sigma R_{\alpha})(V_{\alpha}) \tag{3.6}$$

$$\Sigma I_{\gamma} = K'(\Sigma R_{\gamma})(V_{\gamma}) \tag{3.7}$$

Besides,

$$V_{\alpha} + V_{\gamma} + V_{c} = 1 \tag{3.8}$$

Where, V<sub>c</sub> is the volume fraction of other phase.

Assume only  $\alpha$  and  $\gamma$  phases exist in the specimen, the equation (3.8) is,

$$V_{\alpha} + V_{\gamma} = 1 \tag{3.9}$$

The relationship between  $V_{\alpha}$  and  $V_{\gamma}$  from the equation (3.6) and (3.7) can be expressed by the next equation,

$$V_{\alpha} = \left[ \sum I_{\alpha} \cdot \sum R_{\gamma} / \sum I_{\gamma} \cdot \sum R_{\alpha} \right] \times V_{\gamma}$$
(3.10)

Solving the equation (3.9) and the equation (3.10) to obtain the volume fraction of austenite which relates to the diffraction peak intensity and R values, the following equation is finally given,

$$V_{\gamma} = \frac{1}{[1 + (\alpha \Sigma I_{\alpha} \cdot \Sigma R_{\gamma} / \Sigma I_{\gamma} \cdot \Sigma R_{\alpha})]}$$
(3.11)

For the determination of the amount of austenite, R values must be obtained by equation (3.3), and I $\alpha$  and I $\gamma$  values by measuring the areas under the diffraction peaks of  $\alpha$  and  $\gamma$ . Resultantly, the volume fraction of austenite (V $\gamma$ ) is attained numerically.

### 3.5.2 Equipment and Measuring Condition

The quantitative measurement of  $V\gamma$  is carried out using X-ray diffraction method which was developed for steel by R.L. Miller and then for high chromium white iron by C. Kim [5]. The measuring condition is demonstrated in Table 3.5. In this experiment, the simultaneously rotating and swinging sample stage was employed to cancel the influence of preferred orientation or textural configuration of austenite in the cast iron. The sample stage is shown in Fig.3.2. Fig.3.3 illustrates the results of preliminary tests using the same specimens as this experiment to prove the

advantage of using of this sample stage. It is evident that the peaks of  $\gamma$ 220 and  $\gamma$ 311 are stronger in the specimen with rotating and swinging (a) than those in the both cases of only rotating (b) and of without rotating and swinging (c). On the other hand, the peaks of  $\alpha$ 200 and  $\alpha$ 220 are weak when the sample stage with rotating and swinging is used. However, the  $V_{\gamma}$  calculated from the diffraction pattern measured using the rotating and swinging sample stage is higher than the other cases. It is because the rotating and swinging could cancel the preferred orientation or texture of austenite. This sample stage is used in this research.

For this investigation, the test piece was prepared by grinding surface and followed by polishing it in the same way as the test piece for microphotography. Mo-K $\alpha$  characteristic line with a wavelength of 0.007 nm (0.711 A°) was used as a source of X-ray beam.

Table 3.5 Condition of X-ray diffraction to measure the volume fraction of retained austenite

Target metal	Мо
Tube Voltage · Current	50 kV · 30mA
Slits	Divergence Slit: 1°, Receiving Slit: 1.5 mm, Scattering Slit: 1°
Filter	Zr
Scanning Range	24-44 deg
Scanning Speed	0.5 deg/min
Step/Sampling	0.01 deg

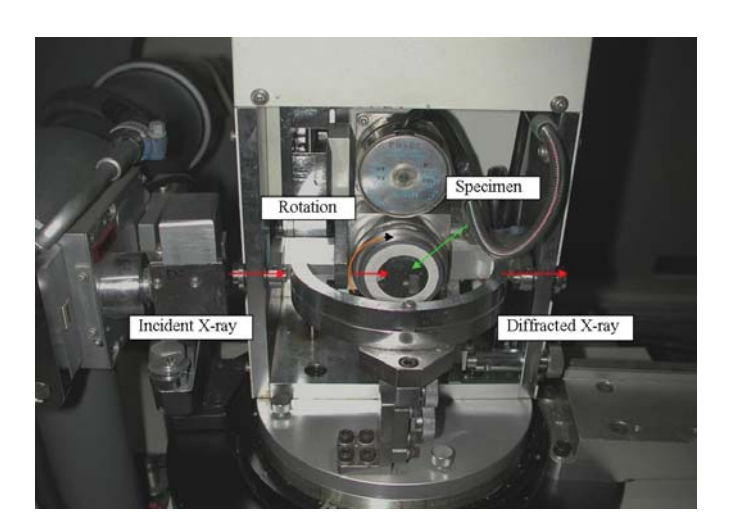


Fig. 3.2 Photograph of special sample stage for retained austenite measurement by X-ray diffraction.

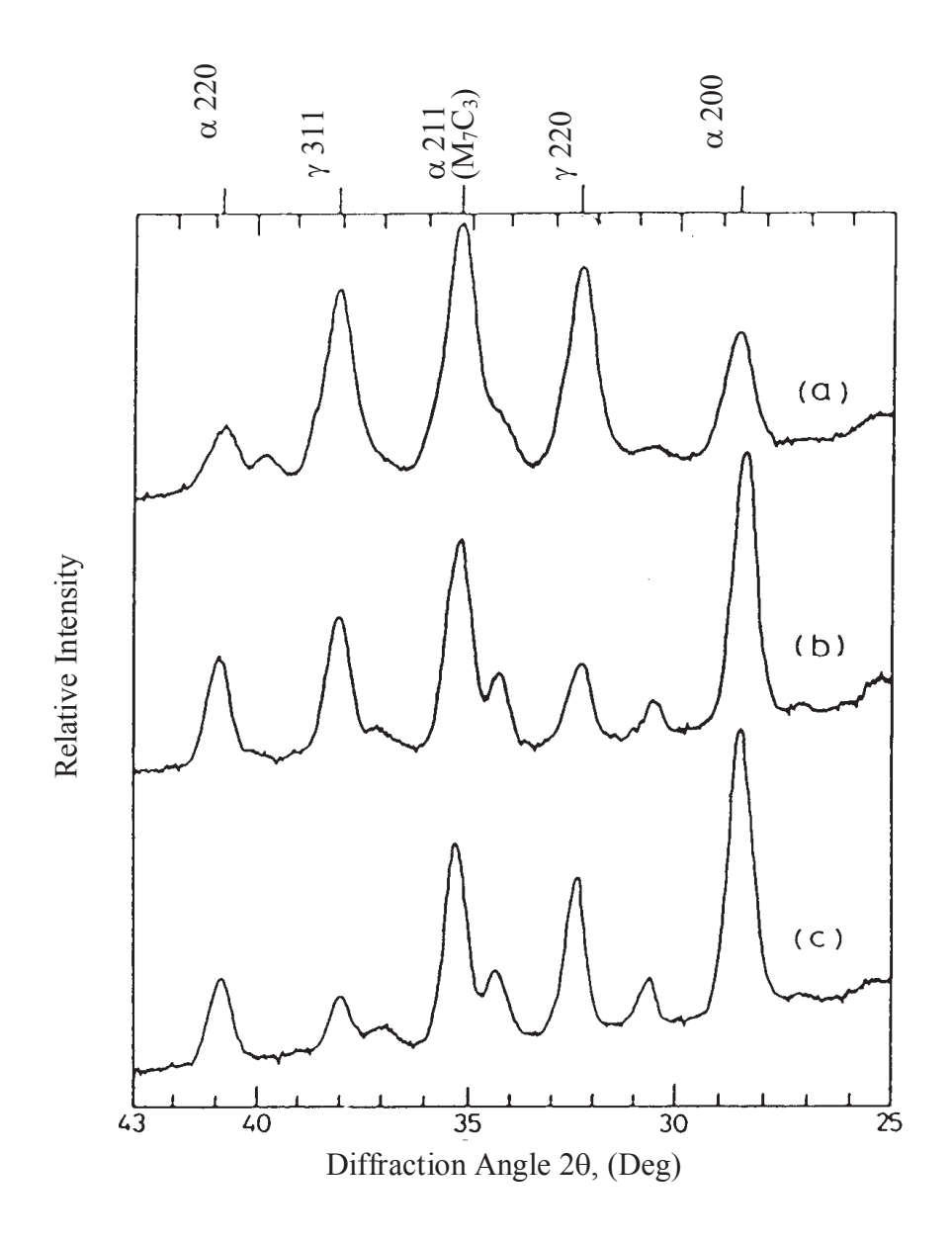


Fig. 3.3 Effect of sample stage condition on diffraction pattern and volume fraction of retained austenite ( $V\gamma$ ) calculated.

### 3.5.3 Calculation of Volume Fraction of Austenite

In this investigation, the crystal planes of peaks adopted for the calculation are (200), (220) of ferrite or/and martensite and (220), (311) of austenite because these four peaks are independent or not interfering from peaks of other phases like carbides. The diffraction patterns of three specimens with different V $\gamma$  are shown for comparison in Fig.3.4 Reason why the  $\alpha_{211}$  peak in these patterns is not taken into account is that this peak is overlapped with a strong peak of chromium carbide. The integrated areas of these peaks are obtained using an image analyzer (Nireco Model Luzex IIIU). The calculation of V $\gamma$  is done by the three combination of peaks,  $\alpha_{200} - \gamma_{311}$ ,  $\alpha_{200} - \Sigma \gamma(220,311)$  and  $\Sigma \alpha(200,220) - \gamma_{311}$ . The average of values calculated from three combinations is plotted.

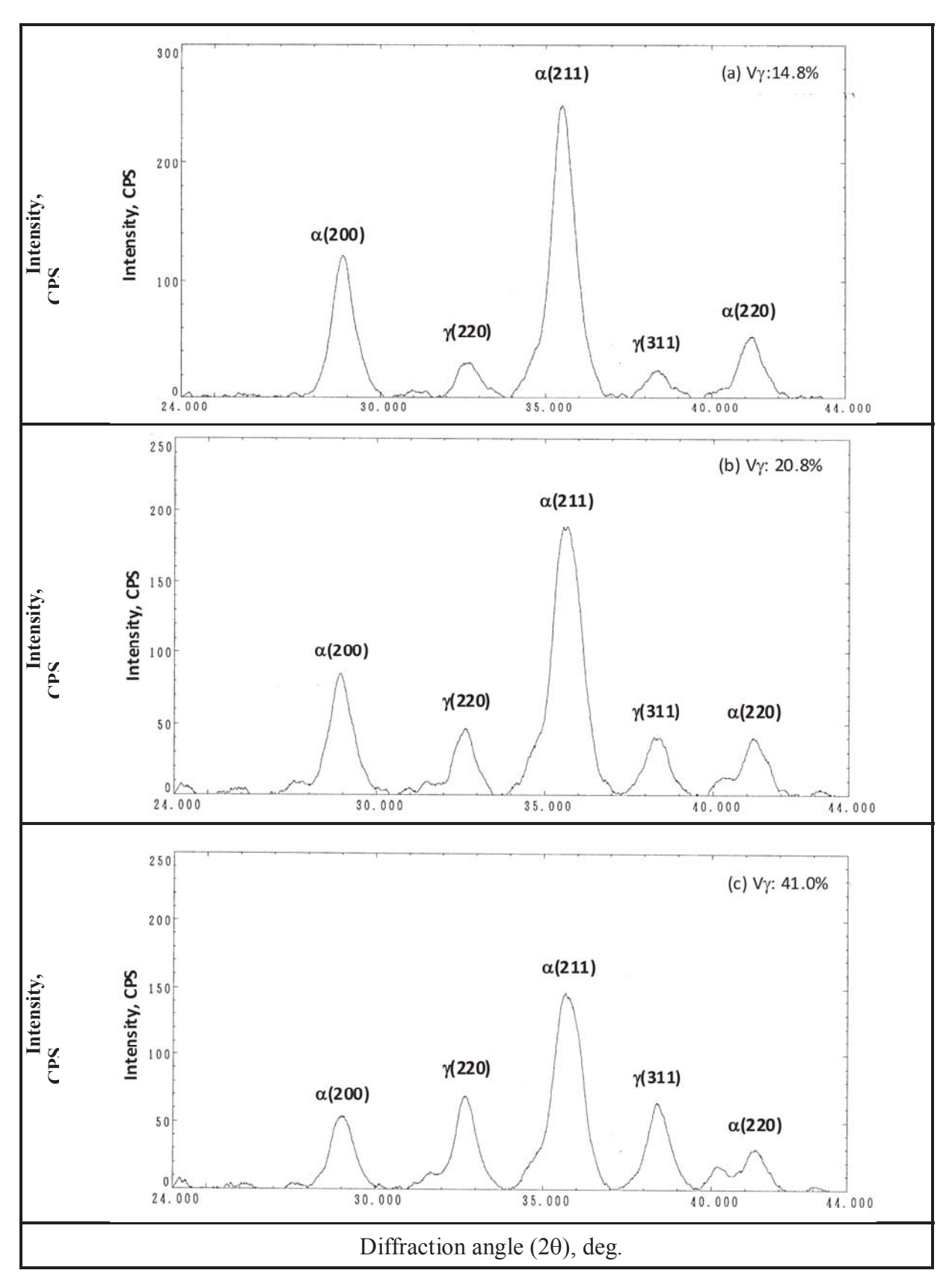


Fig.3.4 X-ray diffraction patterns of specimens with different volume fraction of retained austenite (V $\gamma$ ): (a) 14.8%, (b) 20.8%, (c) 41.0%.

### 3.6 Abrasion Wear Test

# 3.6.1 Suga abrasive wear test

The surface roughness of test pieces are controlled less than 3µm using a grinding machine. The surface roughness is measured at three location using a roughness tester. A schematic drawing of Suga wear tester is illustrated in Fig.3.5. Under a load of 10 N (1kgf), the abrading wheel (44 mm in diameter and 12 mm in thickness) fixed by a 180 mesh SiC abrasive paper on the circumference is revolved intermittently, moving back and forth for 30 mm per one stoke on a same area of the test piece in dry condition. The revolving speed of the abrading wheel is 0.345 mm/s and the worn area is 360 (12x30) mm². The abrading wheel rotates 0.9 degree by every one stroke. Therefore, it completely rotates one revolution or 360 degree after moving back and forth for 400 strokes. After testing, the specimen is cleaned with acetone in an ultrasonic cleaner and then dried. The weight loss of the test piece is measured using a high precision digital balance with 0.1 mg accuracy. The test is repeated up to eight times for one test piece.

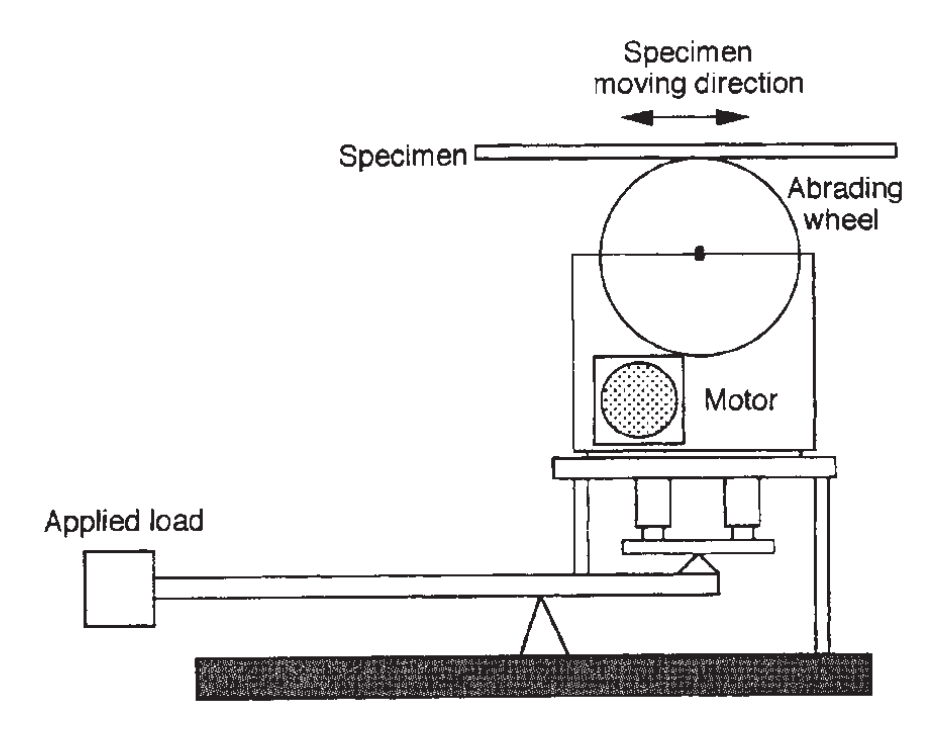


Fig.3.5 Schematic drawing of Suga abrasion wear tester.

### 3.6.2 Rubber Wheel abrasion wear test

The schematic drawing of Rubber Wheel abrasion wear tester is shown in Fig. 3.6. The silica sand of AFS 60 grade is used as the abrasives. The sands are fed to the contacting face between the rotating rubber wheel with 250 mm in diameter and test piece. The test is conducted at a rotating speed of 120 rpm. The rate to feed the abrasives is approximate 250-300 g/min. The load applied is 8.7 kgf. After the rubber wheel rotates for 1,000 revolutions or at wear distance 785.5 m, the specimen is got off and cleaned in an ultrasonic acetone and then dried. The weight of the test piece is measured using a high precision digital balance with 0.1 mg accuracy. The test is repeated four times or up to the wear distance 3142 m per one test piece.

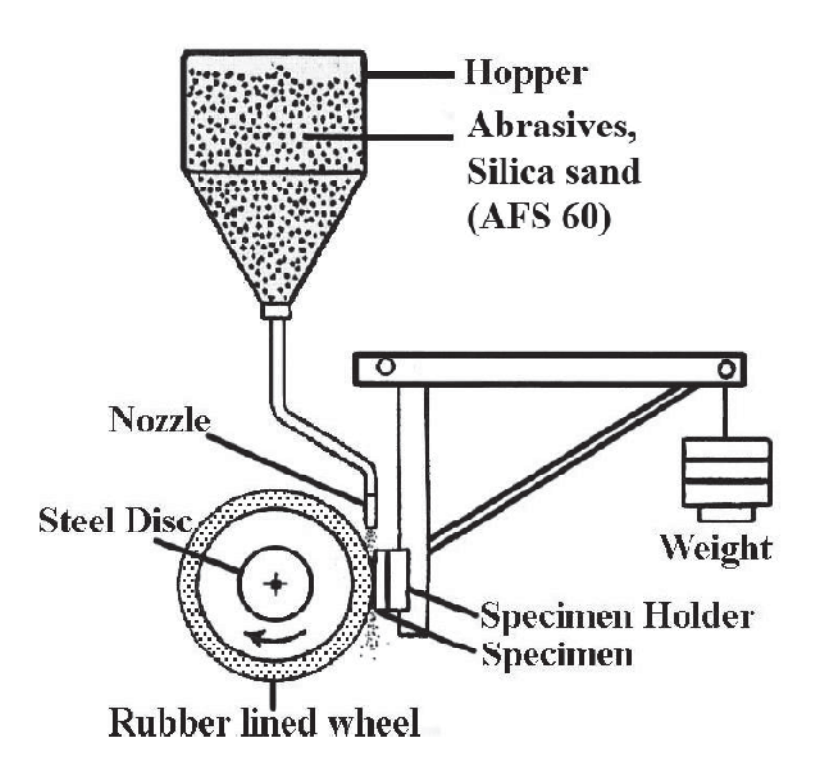


Fig. 3.6 Schematic drawing of Rubber Wheel abrasion wear tester. [8]

## Chapter 4

## **Experimental Results and Discussions**

# 4.1 Characterization of test specimen

#### 4.1.1 As-cast state

As a typical, microphotographs of 26% Cr cast irons without and with Mo are shown in Fig. 4.1. Every microstructure consists of primary dendrite and (γ+M<sub>7</sub>C<sub>3</sub>) eutectic structure. The morphology of (γ+M<sub>7</sub>C<sub>3</sub>) eutectic is similar to each other but the sizes of eutectic colony and eutectic carbide particle are different. It is found that the carbide particle size gets coarser with an increase in Mo content. Mo is a strong carbide forming element and it forms Mo<sub>2</sub>C (M<sub>2</sub>C) carbide during solidification. It was reported that the M<sub>2</sub>C eutectic carbides precipitate with 2% Mo at the boundary of eutectic colonies in 20% Cr cast iron.<sup>3</sup> In this experiment, the M<sub>2</sub>C eutectic carbide could precipitate from the melt with Mo more than 2% that it can be found from the SEM microphotographs. Mo is simultaneously distributed into matrix and affects its transformation. The matrix all specimens are all austenitic and possibly some martensite may exist there. This is explained by the fact that Mo delays pearlite transformation and lowers the Ms temperature.

Effect of Mo content on hardness and  $V\gamma$  of as-cast specimens is shown in Fig. 4.2. The hardness decreased gradually with an increase in Mo. The change in microhardness shows a similar behavior to that in macrohardness. The  $V\gamma$  increases gradually as the Mo content increases. Here, it can be concluded that an increase in  $V\gamma$  and a decrease of martensite by increasing Mo content cause low hardness.

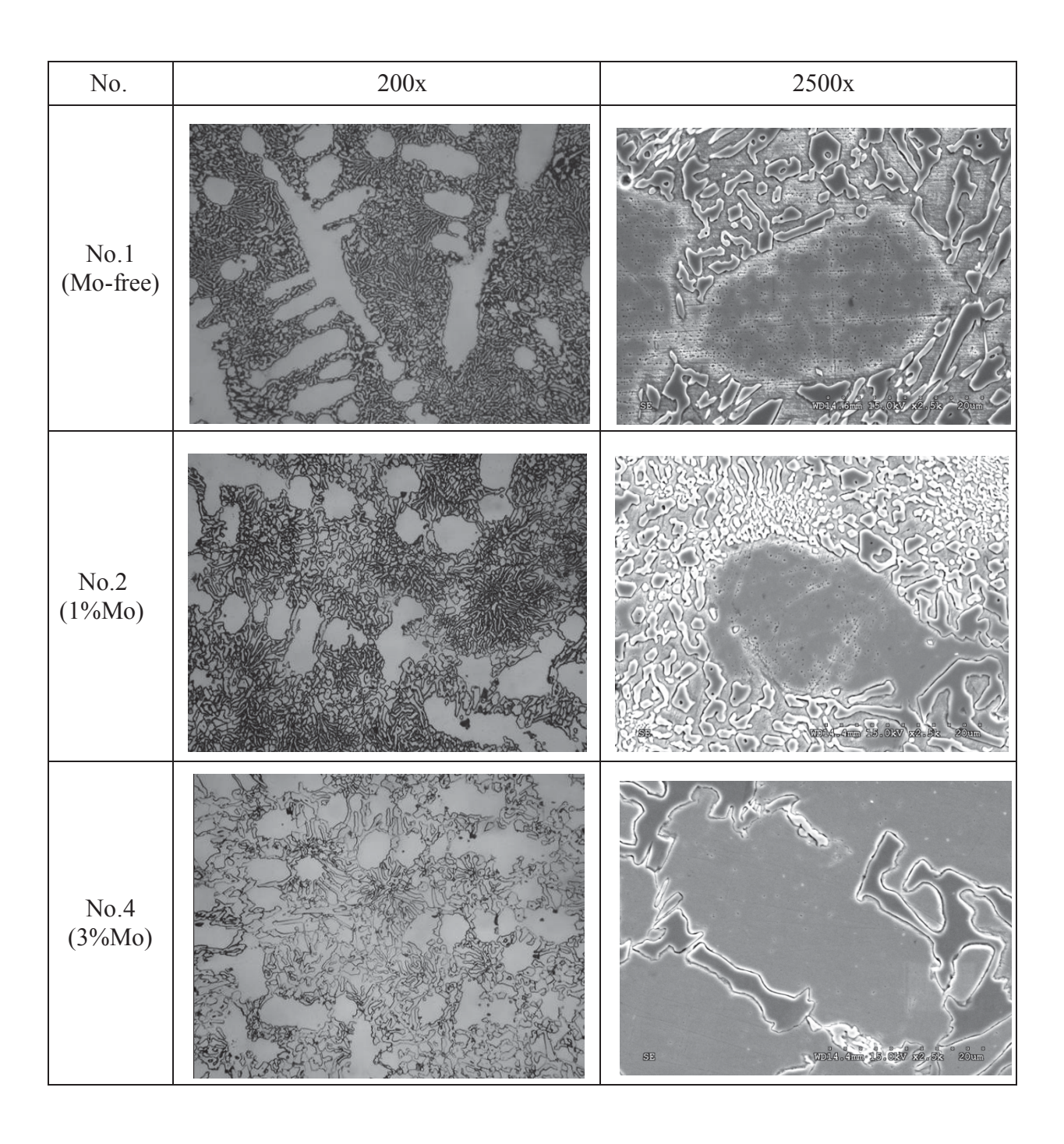


Fig. 4.1 Microphotographs of as-cast hypoeutectic 26% Cr cast irons without and with Mo.

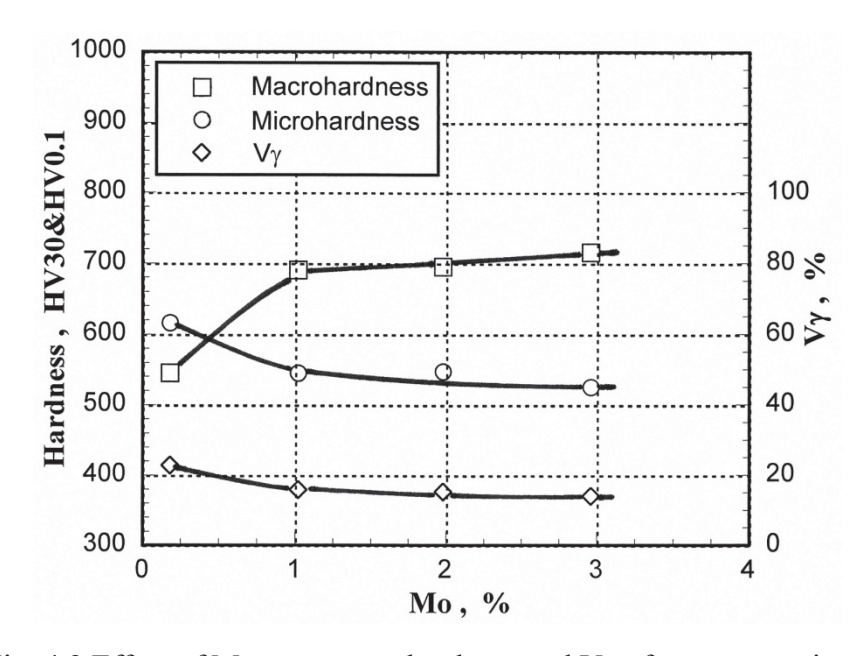


Fig. 4.2 Effect of Mo content on hardness and Vγ of as-cast specimens.

### 4.1.2 Heat treatment state

The as-hardened microstructures of 26% Cr cast irons with and without Mo are shown in Fig. 4.3. The matrix structure consists of a large number of fine precipitated carbides, martensite and retained austenite. It was reported that the secondary carbides which precipitated in the as-hardened state of high chromium cast irons are mostly M<sub>7</sub>C<sub>3</sub> carbides co-existing with M<sub>23</sub>C<sub>6</sub> carbides.<sup>1,3)</sup> The retained austenite which existed more in the as-cast state is destabilized to precipitate fine secondary carbides during holding at the austenitizing temperature, and then transforms into martensite during cooling.

Hardness and  $V_{\gamma}$  of test specimens are summarized in Table 4.1. These test pieces with different hardness and  $V_{\gamma}$  were supplied to the abrasive wear test. It is found that hardness and the  $V_{\gamma}$  change depending on the heat treatment condition and Mo content. The  $V_{\gamma}$  in the as-hardened state is higher than that in the tempered state, and it is clear that the  $V_{\gamma}$  value of L-H<sub>Tmax</sub> specimen is greater than those of H<sub>Tmax</sub> and H-H<sub>Tmax</sub> specimens.

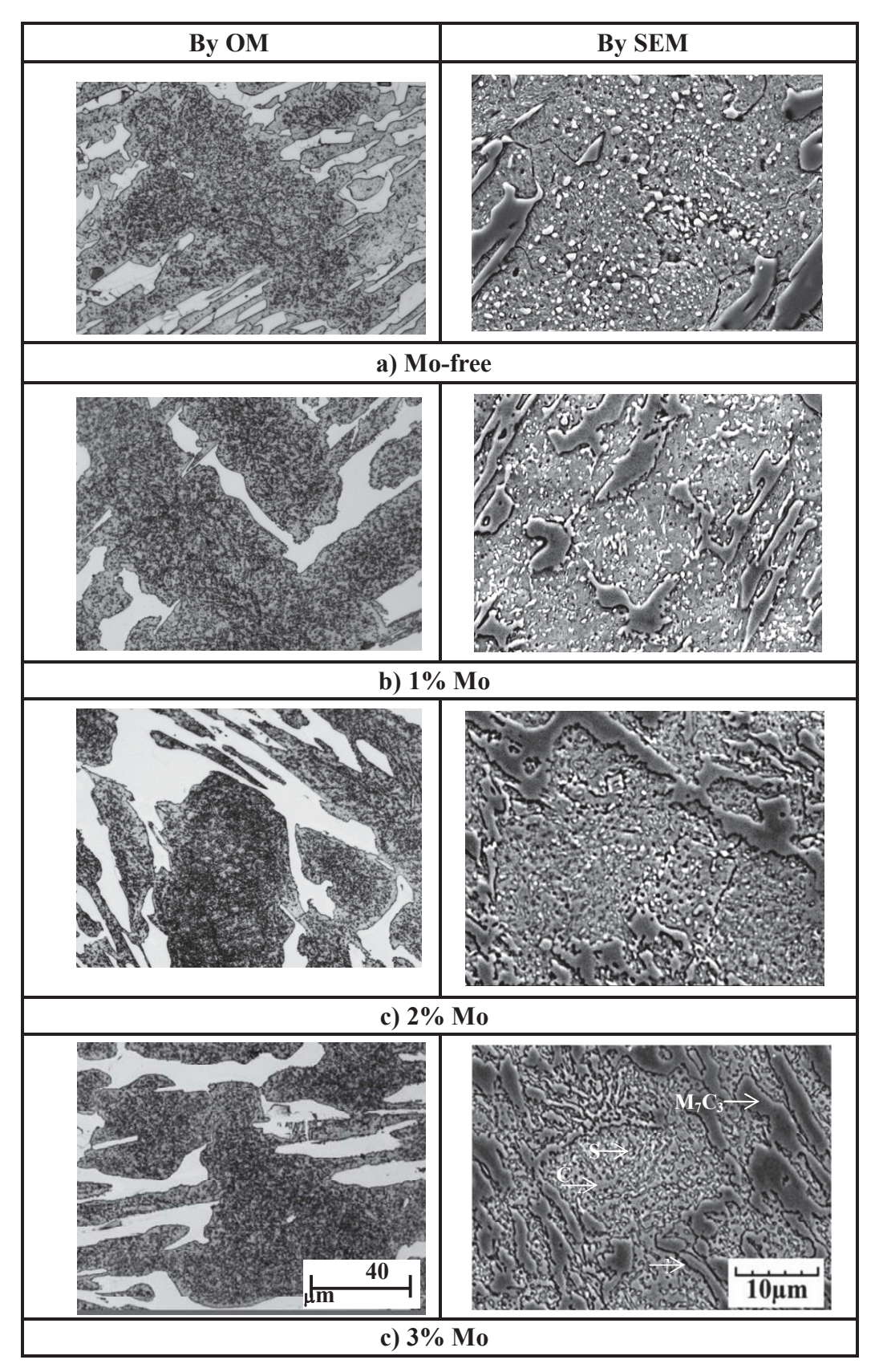


Fig. 4. 3 As-hardened microstructures of hypoeutectic 26% Cr cast irons without and with Mo.

(A: Austenite, M: Martensite, SC: Secondary carbide)

Table 4.1 Hardness and volume fraction of retained austenite  $(V_{\gamma})$  of specimens with different heat treatment conditions.

Specimen		Macro-hardness	Micro-hardness	<b>T</b> 7 0/
Mo content	Heat treatment condition	(HV30)	(HV0.1)	$V_{\gamma}$ , %
	As-hardened	810	755	6
Ma fraa	L-H <sub>Tmax</sub> (673 K)	743	724	4
Mo-free	H <sub>Tmax</sub> (723 K)	769	741	2
	H-H <sub>Tmax</sub> (773 K)	751	726	1
	As-hardened	865	762	8
1% Mo	L-H <sub>Tmax</sub> (673 K)	782	737	5
	H <sub>Tmax</sub> (748 K)	818	752	4
	H-H <sub>Tmax</sub> (800 K)	714	636	1
	As-hardened	898	816	16
20/ M-	L-H <sub>Tmax</sub> (673 K)	845	757	9
2% Mo	H <sub>Tmax</sub> (748 K)	866	780	5
	H-H <sub>Tmax</sub> (800 K)	854	768	4
	As-hardened	873	780	16
20/ 1/4	L-H <sub>Tmax</sub> (673 K)	831	766	9
3% Mo	H <sub>Tmax</sub> (748 K)	835	768	7
	H-H <sub>Tmax</sub> (823 K)	710	616	4

# 4.2 Suga abrasive wear test

# 4.2.1 Relationship between wear loss and wear distance

In this experiment, series of heat-treated specimens shown in Table 4.1 were used. The relationship between wear loss and wear distance by Suga wear tester of all specimens is presented in Fig. 4.4 - 4.7, respectively. In all of the figures, the wear loss increases in proportion to the wear distance. Total wear losses of specimens with different heat treatment condition at about 192 m wear test are summarized in Table 4.3. Since the linear relations were obtained between wear loss and wear distance in all the specimens, the parameter of wear rate (Rw) which is expressed by the slope of each straight line is introduced. The Rw values of all the specimens are summarized in Table 4.4. It is found that the Rw varies by the heat treatment condition and Mo content.

Table 4.3 Total wear loss at 192 m of Suga abrasion wear test with a load of 9.8 N (1 kgf) for specimens with and without Mo.

Specimen	Total wea	ar loss by Suga	wear test at 192	m, mg.
T T	As-hardened	L-H <sub>Tmax</sub>	$H_{Tmax}$	H-H <sub>Tmax</sub>
Mo-free	74.4	79.9	75.9	82.1
1% Mo	73.7	78.0	71.2	81.9
2% Mo	65.9	68.2	70.1	74.7
3% Mo	71.9	74.2	68.3	78.7

Table 4.4 Wear rate (Rw) by Suga abrasion wear test (two-body-type) of heat-treated specimens with different Mo content. Load: 9.8 N(1kgf).

	Wear rate (Rw), mg/m			
Specimen	As-hardened	L-H <sub>Tmax</sub>	$H_{Tmax}$	H-H <sub>Tmax</sub>
Mo-free	0.39	0.42	0.40	0.43
1% Mo	0.38	0.41	0.37	0.43
2% Mo	0.34	0.35	0.36	0.38
3% Mo	0.37	0.38	0.35	0.41

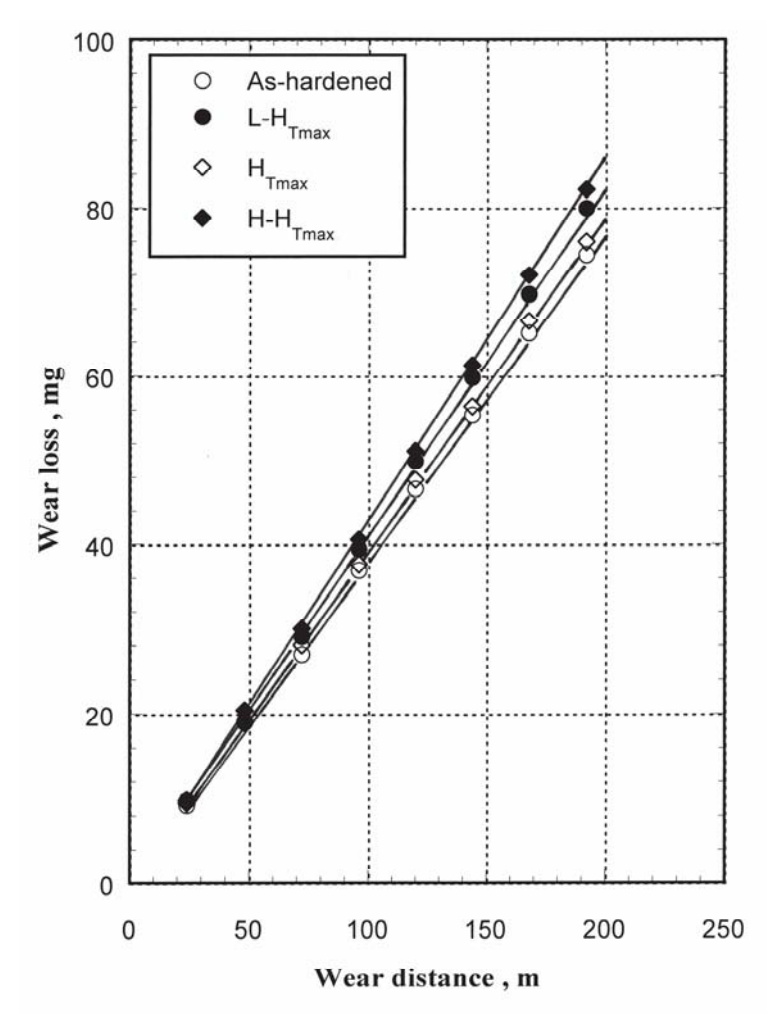


Fig. 4.4 Relationship between wear loss and wear distance of heat-treated 26%Cr cast irons without Mo by Suga wear test.

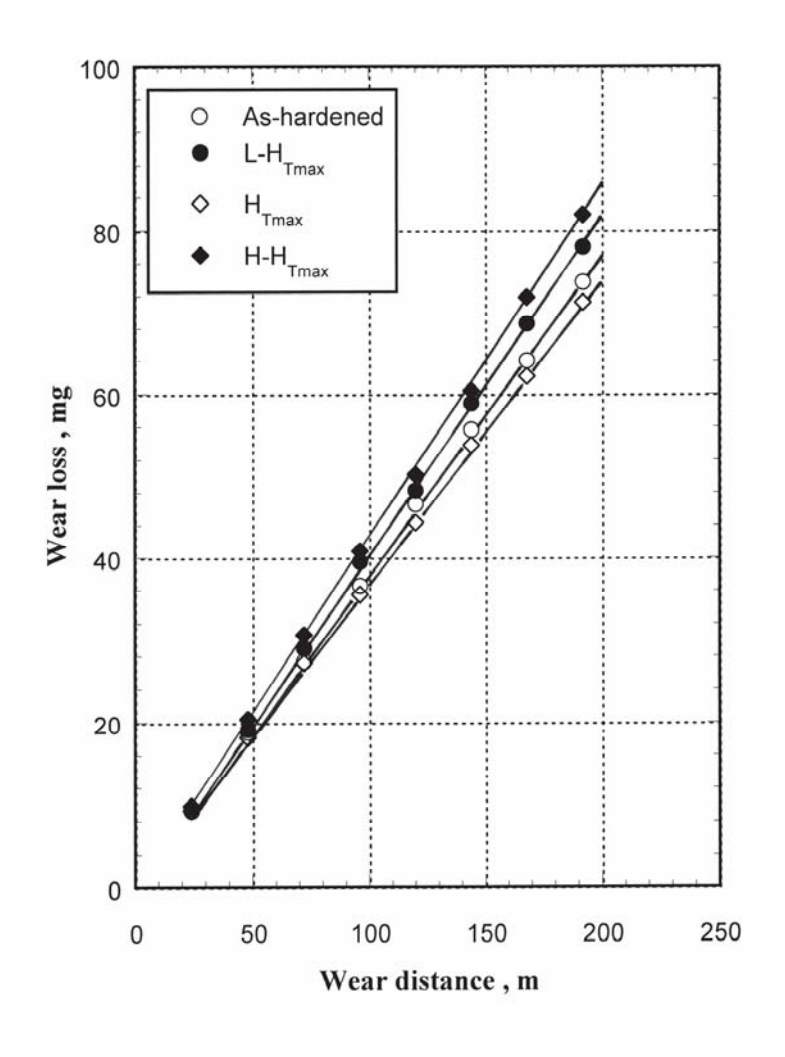


Fig. 4.5 Relationship between wear loss and wear distance of heat-treated 26%Cr cast irons with 1% Mo by Suga abrasive wear test.

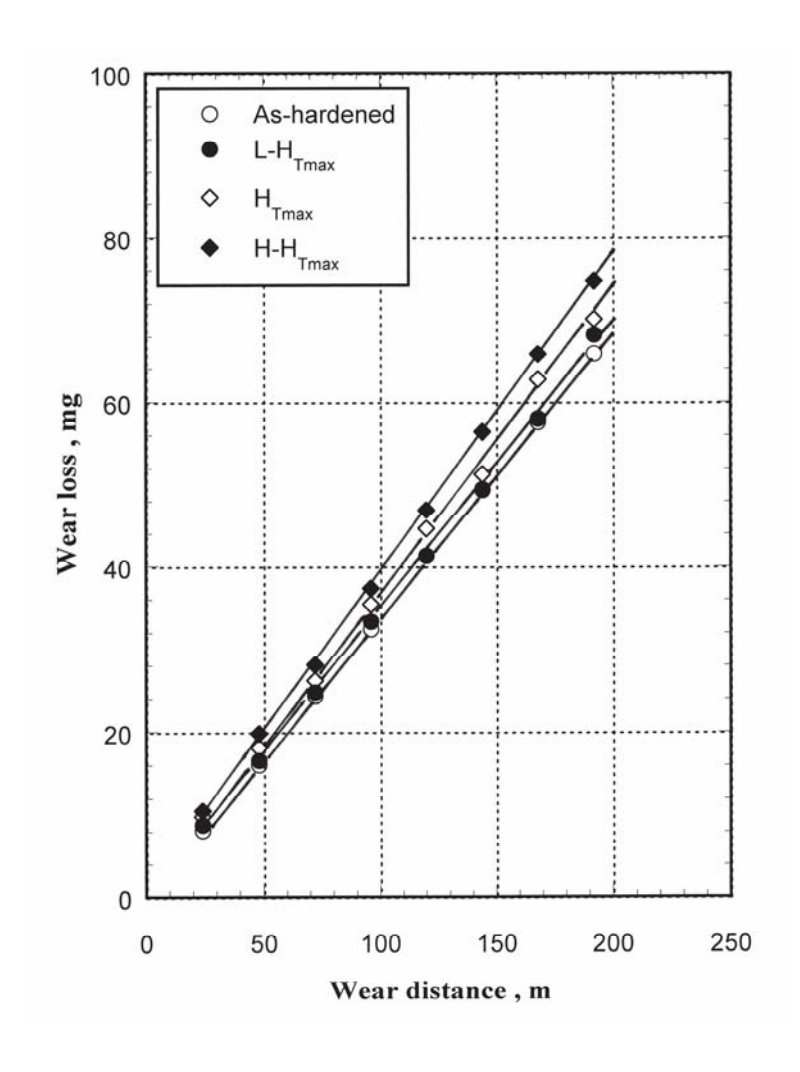


Fig. 4.6 Relationship between wear loss and wear distance of heat-treated 26%Cr cast irons with 2% Mo by Suga abrasive wear test.

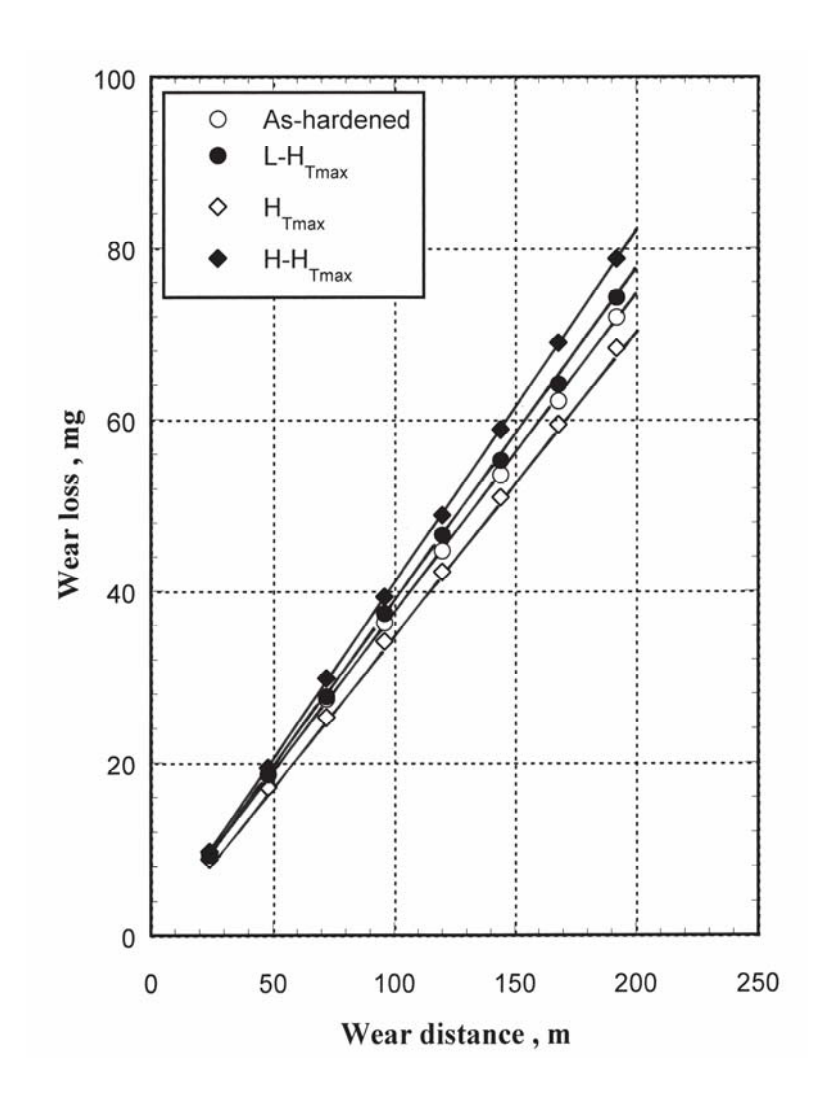


Fig. 4.7 Relationship between wear loss and wear distance of heat-treated 26%Cr cast irons with 3% Mo by Suga abrasive wear test.

### 4.2.2 Relationship between wear rate (R<sub>W</sub>) and hardness

In this study, the effects of macro-hardness on the wear rate ( $R_W$ ) of Suga abrasion wear tests is presented in the Fig.4.8. From this diagrams, it is found that the  $R_W$  decreases proportion to macrohardness, as the macrohardness increases. The relation is expressed by the next equation,

$$Rw = -4.2 \times 10^{-4} \times HV30 + 0.72$$
 (R = 0.88)

It is clear that the more macro-hardness is, the better wear resistance is obtained. In tempered state, therefore the specimen with  $H_{Tmax}$  has the largest wear resistance.

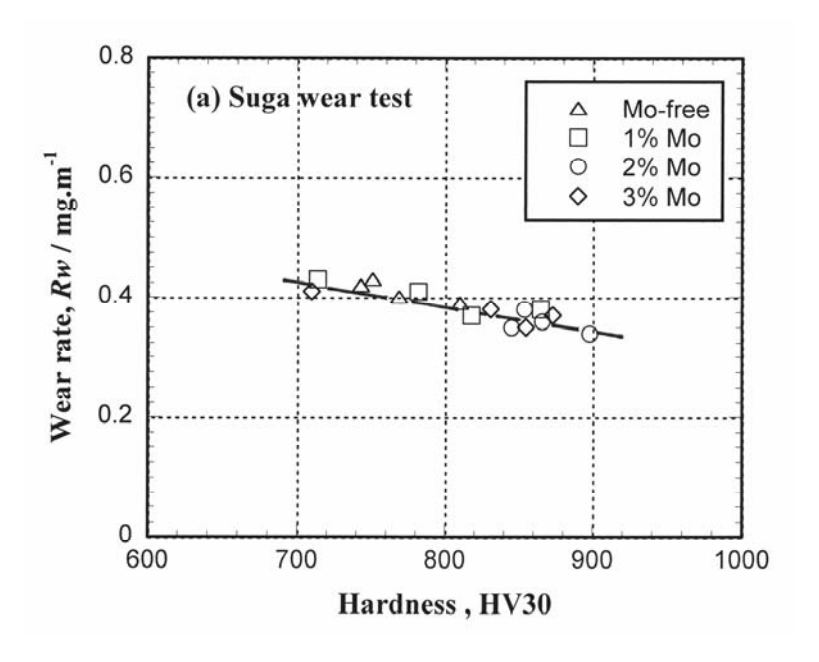


Fig. 4.8 Relationship between wear rate (R<sub>W</sub>) by Suga abrasive wear test and macrohardness of specimens.

# 4.2.3 Relationship between wear rate ( $R_W$ ) and $V_{\gamma}$

The relationship between  $R_W$  and  $V_\gamma$  of tested specimens in Suga abrasive wear test is shown in the Fig.4.9. There appears minimum  $R_W$  at 10-15% $V_\gamma$ . This suggests that a certain amount of  $V_\gamma$  could contribute to improve the abrasive wear resistance. These results agree roughly with the experimental results reported by other work. [7] The  $R_W$  decreases remarkably up to 15% $V_\gamma$  with a decrease in  $V_\gamma$  and over 15% $V_\gamma$ , it increases little as the  $V_\gamma$  increases. The decrease in  $R_W$  until 15% $V_\gamma$  is due to an increase of hard martensite and an increase of  $V_\gamma$  to improve the toughness and the precipitation of secondary carbides of  $M_7C_3$  and  $M_{23}C_6$  in the

matrix. The reason of gradual increase in  $R_W$  when  $V_\gamma$  get over each critical values about 15% $V_\gamma$ , it is due to that an increase in the  $V_\gamma$  promote the work hardening effect by increased martensite transformation and it contributed the wear resistance. In the area of very low  $V_\gamma$ , the  $R_W$  is relatively high in these both two wear tests because matrix is mostly pearlite and coarse secondary carbides.

## 4.2.4 Relationship between wear rate (R<sub>W</sub>) and Mo content

In order to explain the effect of Mo content on the  $R_W$  clearly, the relation of  $R_W$  and  $V_\gamma$  is are expressed by each specimen and they are shown in Fig.4.10. The effect of Mo content on the  $R_W$  is clearly shown and it is found that the  $R_W$  is decreased or wear resistance is increased with increasing Mo content of specimen. It could be explained by the fact that Mo increases the hardness of not only matrix but also eutectic carbide. Under the high stress abrasive wear, the abrasive particles with extremely high hardness (2500-2600 HV) 3) cut through both of the eutectic carbide and matrix. So, an increase in hardness by Mo addition could check the crack propagation, and resultantly, the Rw decreased.

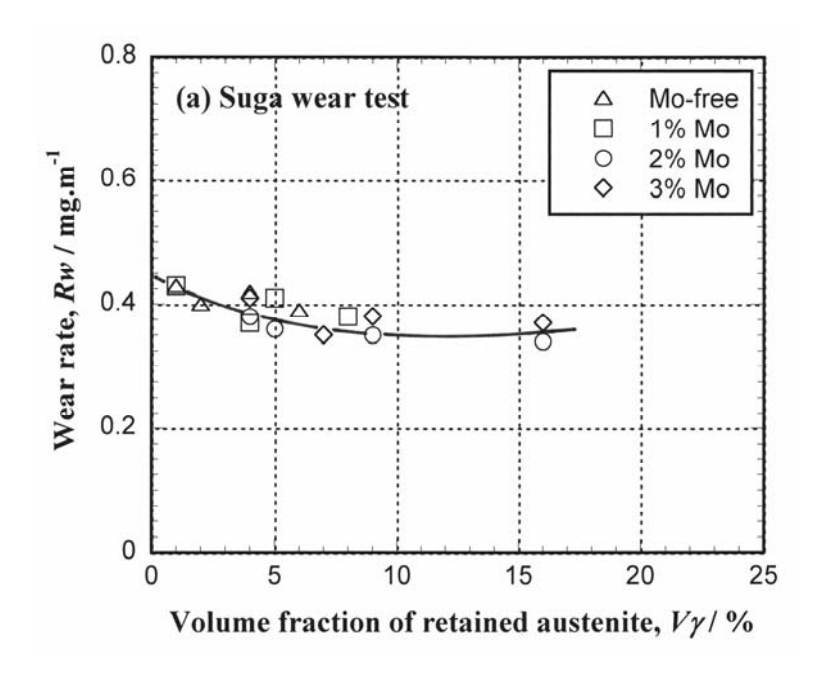


Fig. 4.9 Relationship between wear rate  $(R_W)$  and  $V\gamma$  of specimens.

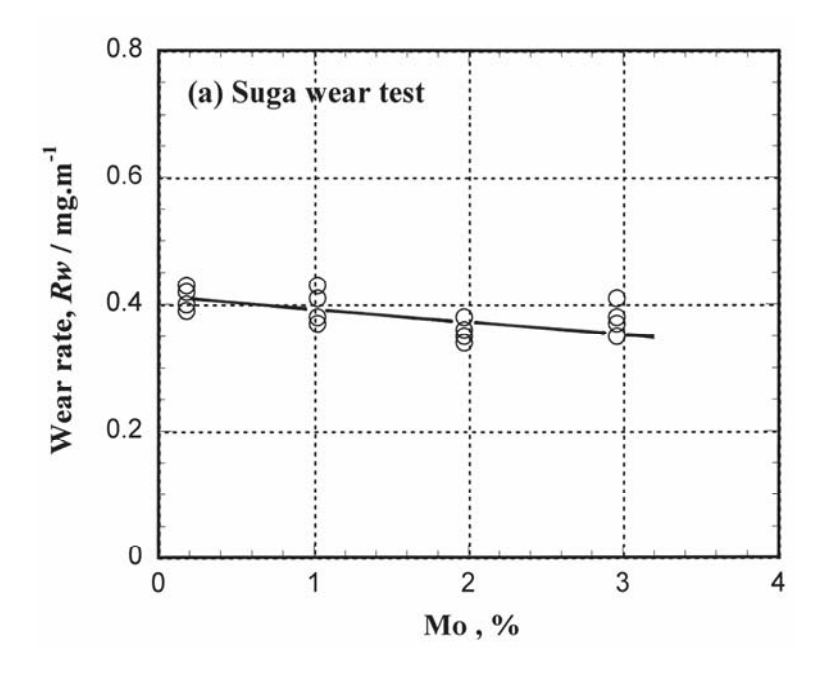


Fig. 4.10 Effect of Mo content on the wear rate (Rw).

### 4.3 Rubber wheel abrasive wear test

# 4.3.1 Relationship between wear loss and wear distance

The results of Rubber Wheel wear tester are displayed in Fig. 4.11-4.14 for specimens with different Mo content, respectively. It is found that the wear loss increased in portion to the wear distance in all the specimens and the relation is shown at the upper part of each figure. The total wear loss and Rw value are correspondingly summarized in Table 4.5 and Table 4.6. It is clear from the results that the smallest Rw is obtained in the as-hardened and  $H_{Tmax}$  specimens. The largest Rw value is obtained in the H-H<sub>Tmax</sub> specimen

Table 4.5 Total wear loss at 3143 m of Rubber Wheel abrasion wear test with a load of 85.3 N (8.7 kgf) for specimens with and without Mo.

Heat	Total wear loss in Rubber Wheel wear test at 3143 m. (mg.)				
Treatment Condition	As-hardened	L-H <sub>Tmax</sub>	$H_{Tmax}$	H-H <sub>Tmax</sub>	
Mo-free	146	208	174	180	
1% Mo	179	213	171	247	
2% Mo	165	177	149	168	
3% Mo	166	203	184	307	

Table 4.6 Wear rate (Rw) by Rubber Wheel abrasion wear test (three-body-type) of heat-treated specimens with different Mo content. Load: 85.3 N (8.7 kgf).

		Wear rate (F	Rw) , mg/m	
Specimen	As-hardened	L-H <sub>Tmax</sub>	$H_{Tmax}$	H-H <sub>Tmax</sub>
Mo-free	0.046	0.067	0.054	0.057
1% Mo	0.056	0.068	0.054	0.078
2% Mo	0.051	0.055	0.047	0.052
3% Mo	0.053	0.066	0.059	0.096

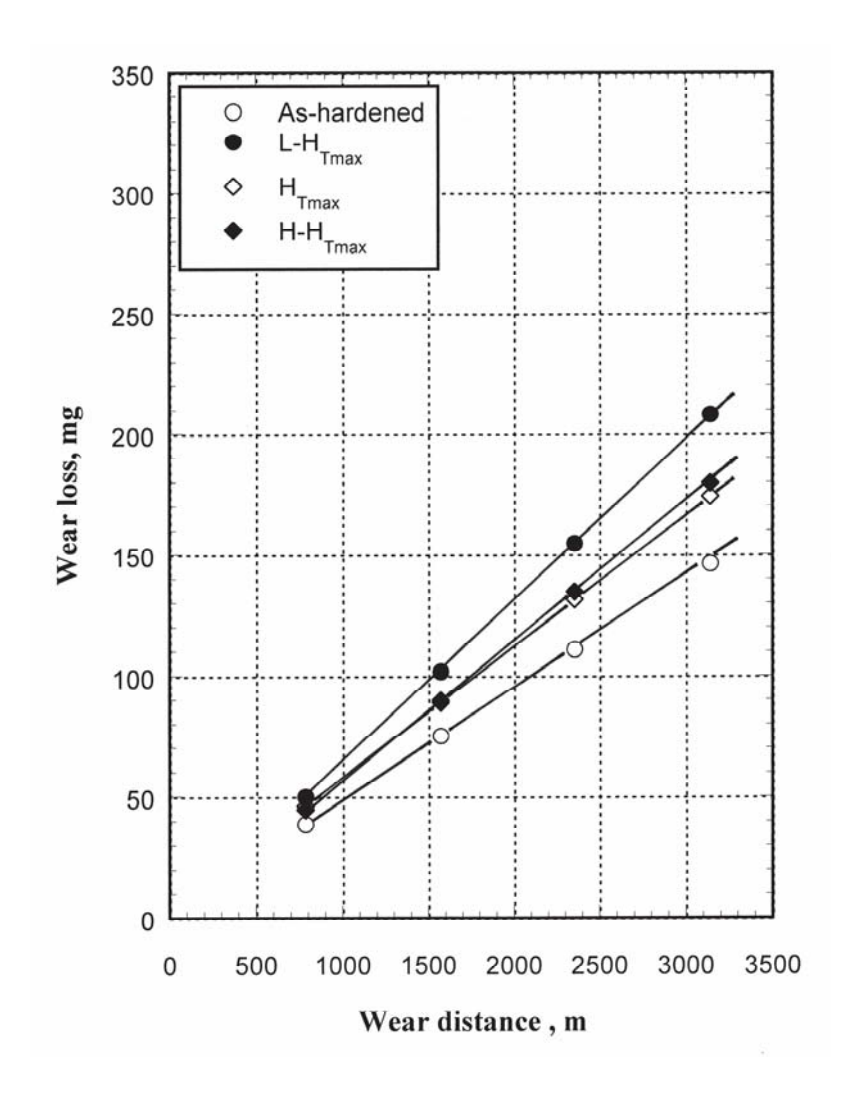


Fig. 4.11 Relationship between wear loss and wear distance by rubber wheel abrasive wear test of 26% Cr cast iron without Mo.

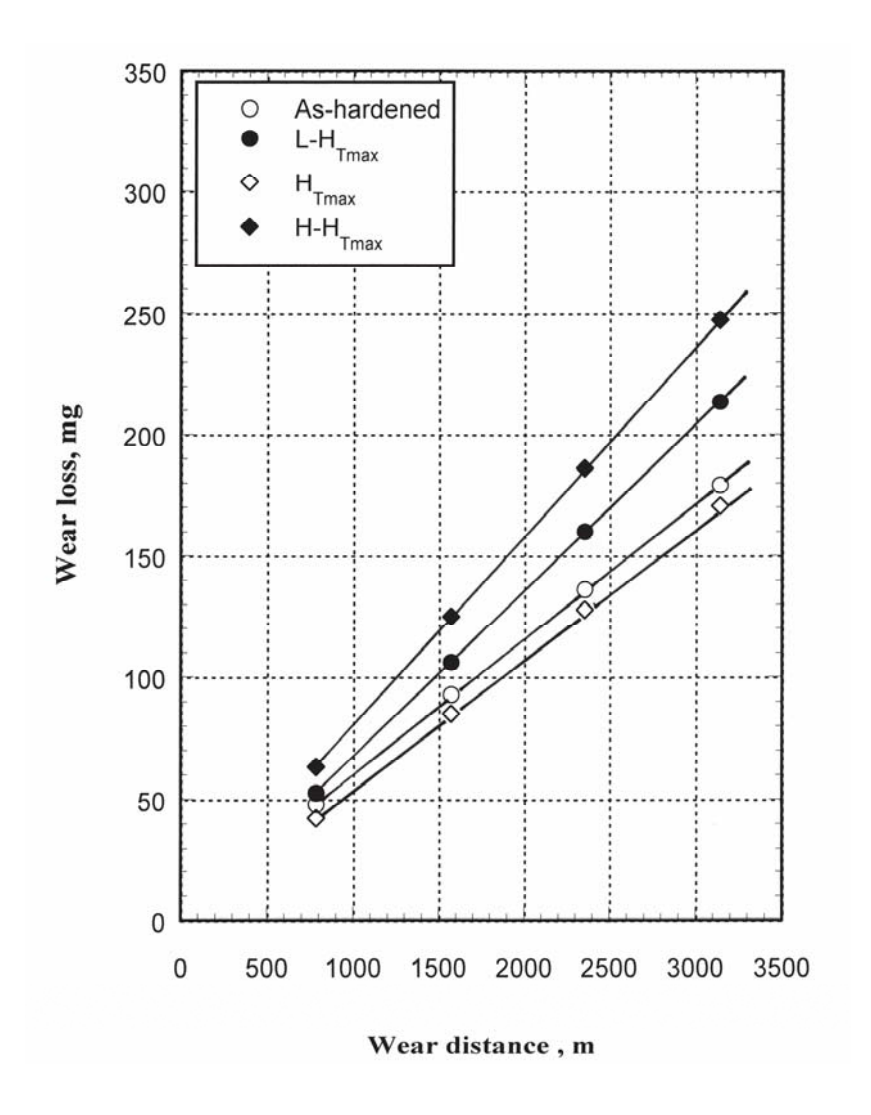


Fig. 4.12 Relationship between wear loss and wear distance by rubber wheel abrasion wear test of 26% Cr cast iron with 1%Mo.

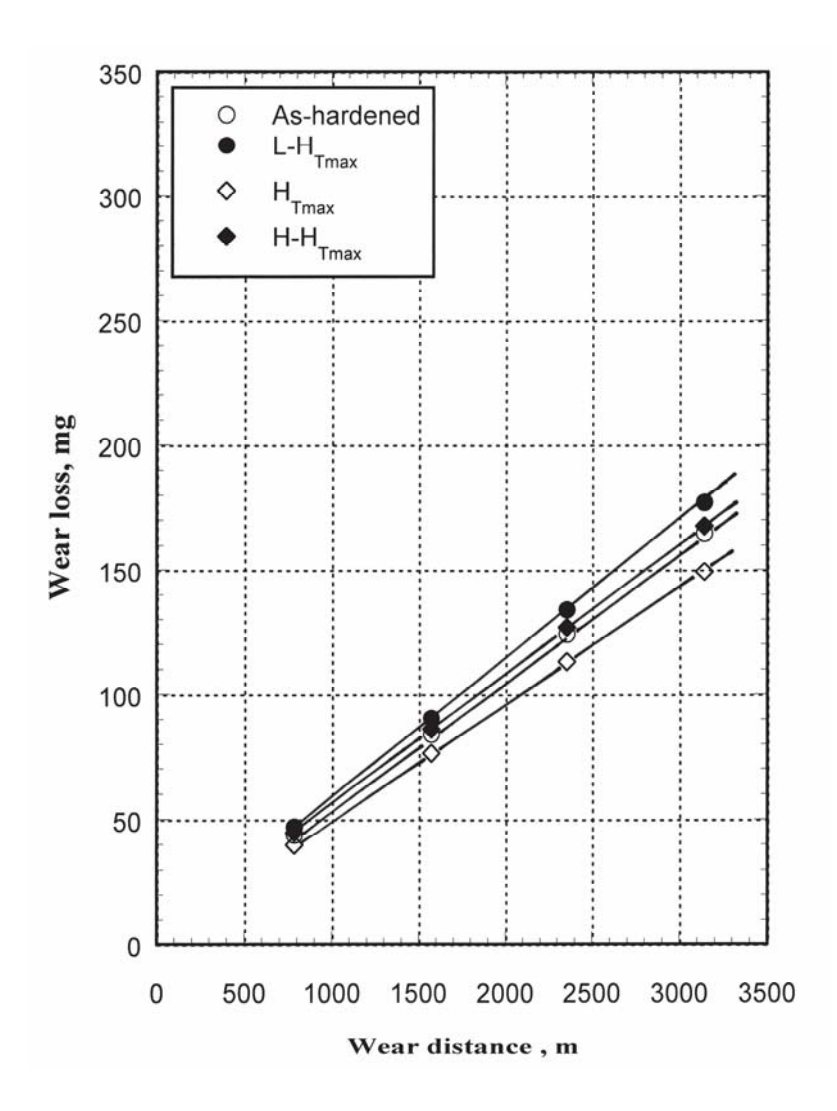


Fig. 4.13 Relationship between wear loss and wear distance by rubber wheel abrasion wear test of 26% Cr cast iron with 2%Mo.

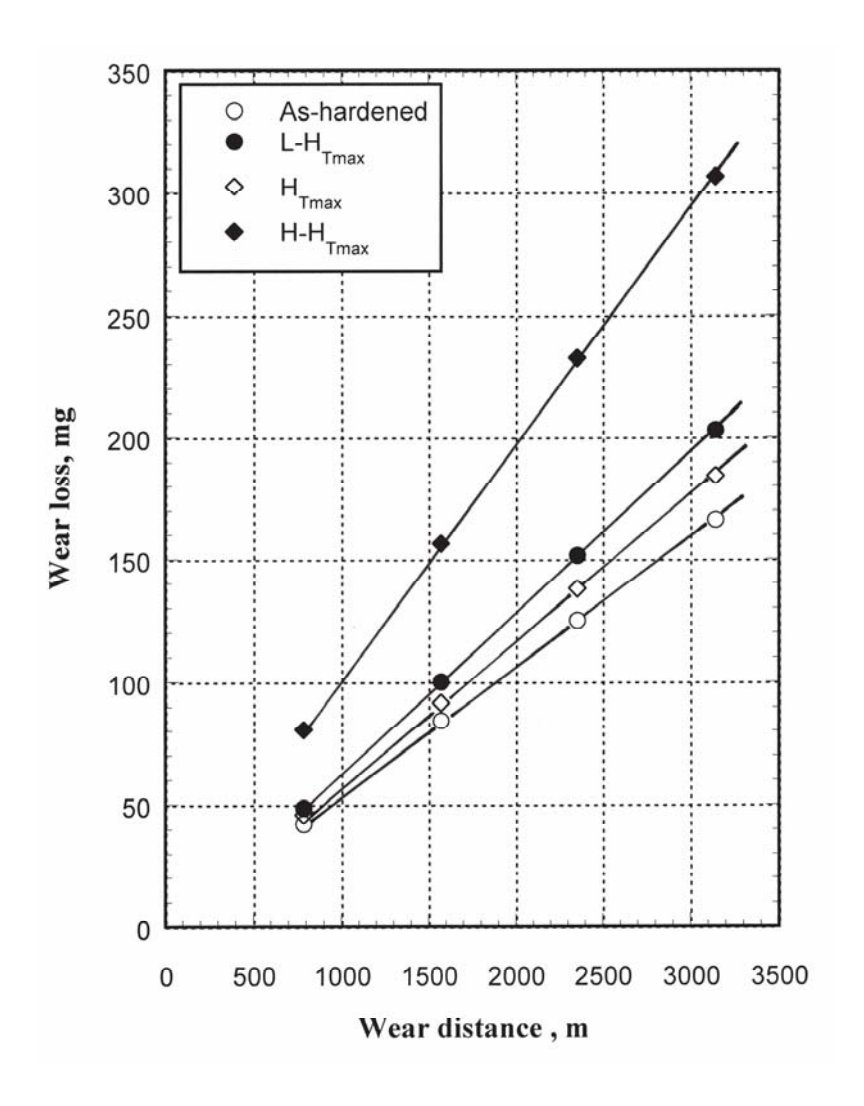


Fig. 4.14 Relationship between wear loss and wear distance by rubber wheel abrasion wear test of 26% Cr cast iron with 3%Mo.

## 4.3.2 Relationship between wear rate (R<sub>W</sub>) and hardness

Relationship betweens Rw and macro-hardness by Rubber Wheel abrasion wear test is shown in Fig. 4.15. The Rw values decrease in proportion to the macro-hardness without scattering regardless of heat treatment condition and Mo content. The relations are expressed by next equations,

$$Rw = -1.6 \times 10^{-4} \times HV30 + 0.19 \qquad (R = 0.73)$$

It is clear from above relations that the higher macro-hardness provides better wear resistance. In order to clarify the sensitivity of hardness, the slopes of lines in Fig. 4.8 for Suga abrasion wear test and in Fig. 4.15 for Rubber Wheel abrasion wear test are calculated. The ratio of is about 2.6. This means that the hardness affected the Rw 2.6 times more in Suga abrasive wear test than that in Rubber wheel abrasive wear test.

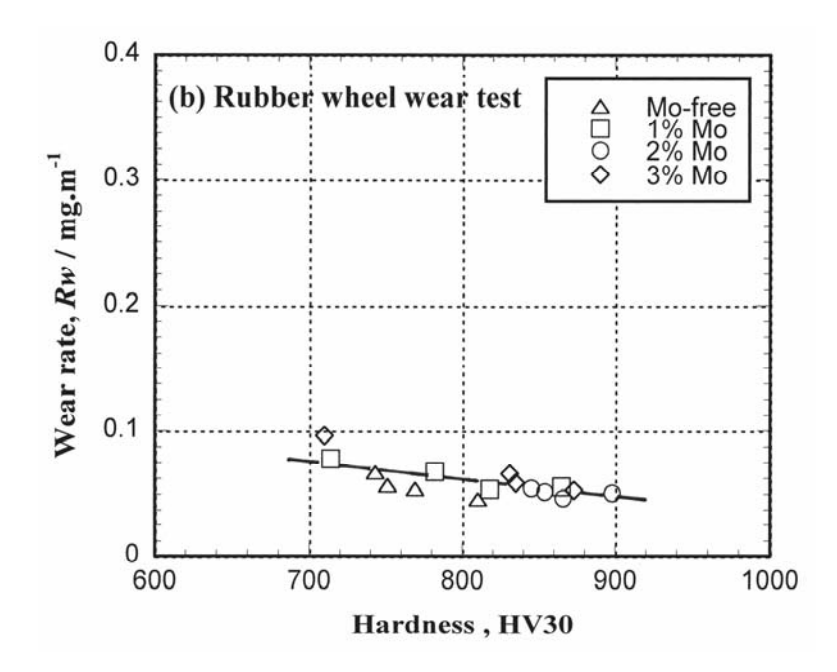


Fig. 4.15 Relationship between wear rate (Rw) and macro-hardness of heat-treated specimens with different Mo content.

# 4.3.3 Relationship between wear rate ( $R_W$ ) and $V_{\gamma}$

The amount of retained austenite also affects the wear resistance of high Cr cast iron. The relationship between Rw and  $V_{\gamma}$  is shown in Fig. 4.16. Though, the data are scattering a little, Rw decreases gradually to the minimum point and then increases again as  $V_{\gamma}$  increases. The equation is as followed;

$$Rw = (2.8x10^{-4}) \times (V\gamma)^{2} - (5.7x10^{-3}) \times (V\gamma) + 0.08 \qquad (R = 0.58)$$

The smallest Rw is obtained at about 10-15%  $V_{\gamma}$ . This suggests that a certain amount of  $V_{\gamma}$  improves the abrasion wear resistance. This result agrees with the results from the other researches using different wear test methods, pin-on-disc test, which is about 20%  $V_{\gamma}$ . [44] The decrease in the Rw with raising the  $V_{\gamma}$  is considered due to the work hardening effect of retained austenite. In the case of very low  $V_{\gamma}$  value, some pearlite possibly appears there which reduces the wear resistance. In the case of high  $V_{\gamma}$  value, excessive retained austenite reduces not only the hardness but also work hardening effect. Resultantly, the Rw increases gradually as the  $V_{\gamma}$  rises.

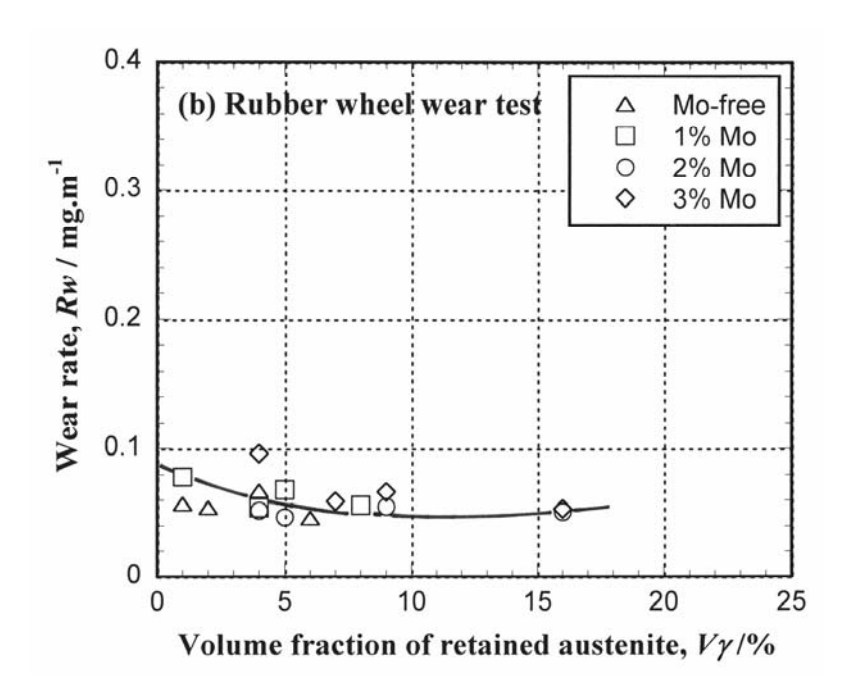


Fig. 4.16 Relationship between wear rate (Rw) and volume fraction of retained austenite ( $V_{\gamma}$ ) of heat-treated specimens with different Mo content.

## 4.3.4 Relationship between wear rate (R<sub>W</sub>) and Mo content

The effect of Mo content on Rw by rubber wheel abrasive wear test is shown in Fig. 4.17. It seems that Mo does not show significant effect on Rw. The Rw values in Rubber Wheel abrasion wear test are little scattered and it seems independent on the Mo content. Although Mo raises the macro-hardness, the Rw values are slightly decreased. This is because the stress concentration on the worn surface is quite low in this test and the hardness of silica sand abrasive particles with about 1200 HV is smaller than that of eutectic M<sub>7</sub>C<sub>3</sub> carbide with 1500-1800 HV. [3] Therefore, the matrix region with lower hardness was preferentially worn by silica sands. It was reported that the removal rate of matrix controls greatly the fracture of carbide and then, the work hardening of austenite is hard to appear effectively because of the low stress concentration. [1,15,17] In this case, the harder matrix provides the better resistance to the abrasive wear. From this viewpoint, it is considered that the matrix could have a major effect on the Rw. In order to explain this result, the micro-hardness of matrices in the test pieces with  $H_{Tmax}$  in Table 4.1 was compared. Looking over the micro-hardness, 741 HV0.1 for Mo-free, 752 HV0.1 for 1%Mo, 780 HV0.1 for 2%Mo and 768 HV0.1 for 3%Mo specimens, it is found that the matrix hardness changes little to an increase in the Mo content. This can support that the Rw varied little by Mo addition, compared with the reasonable change of the Rw in Suga wear test.

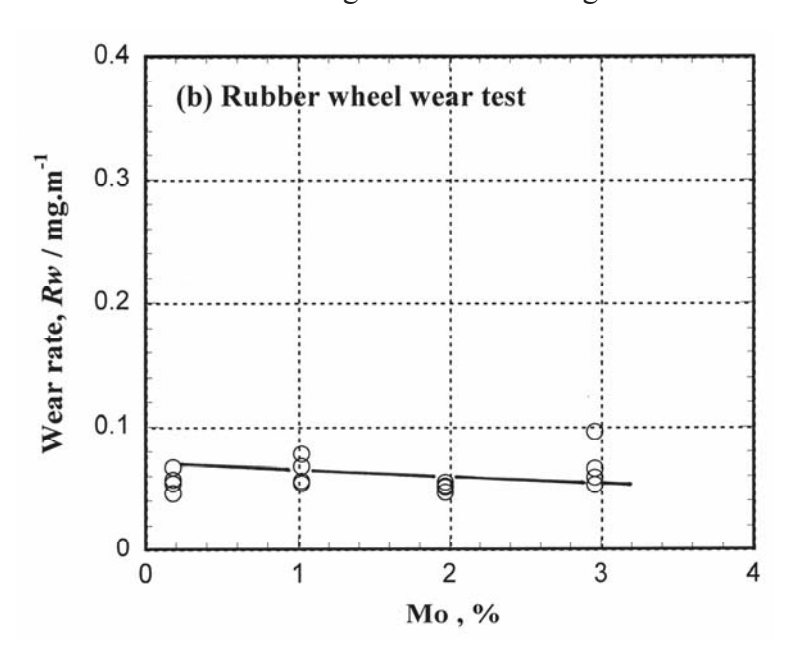


Fig. 4.17 Effect of Mo content on wear rate (Rw) of all the specimens.

### 4.4 Mechanism of Abrasive wear

In order to comprehend the abrasive wear behavior, the worn surface of 1%Mo specimen with  $H_{Tmax}$  was observed by SEM. The representative examples of worn surface appearance are shown in Fig. 4.18. In Suga wear test, the abraded regions showing fine lines caused by scratching correspond to the matrix region. On the microphotographs, it is found that the eutectic carbides are worn very little by scratching and more by spalling or pitting, and that much rougher worn surfaces are formed in the portion of matrix by grooving and tearing. The matrix is preferably shaved or worn and removed more than the eutectic carbides. The crack forms probably in the eutectic carbides because the load concentrates on the carbides. Once the cracks are produced, the spalling of carbides begins to take place. The tearing and grooving were observed because the ductile matrix with austenite can be deformed easily without cracking by the stress of abrasive particles.<sup>3)</sup> Therefore, the grooving is limited in the matrix region and the tearing could originates at the grooves in the matrix.

In Rubber wheel wear test, the lines displaying the wear direction are not observed. This is because the abrasive particles move freely on the surface of test piece. The worn surface consists of the pitting in the matrix region and the scratching in the eutectic area. The matrix removes first followed by the fracture of carbides.

In the cross-sectional microstructures, the worn surface by Suga wear test is smooth and flat. This means that the abrasive particles passed through both of matrix and carbides simultaneously. However, it is also found that the wear of matrix is more violent than that of eutectic carbide, particularly in the primary matrix region. For the specimen of Rubber wheel wear test, the matrix has a concave surface and seems to be worn preferentially compared with the eutectic area, i.e. the matrix removes first followed by the fracture of carbides. It can be said that the removal rate of matrix is related to not only the total wear rate but also the fracture rate of carbide.

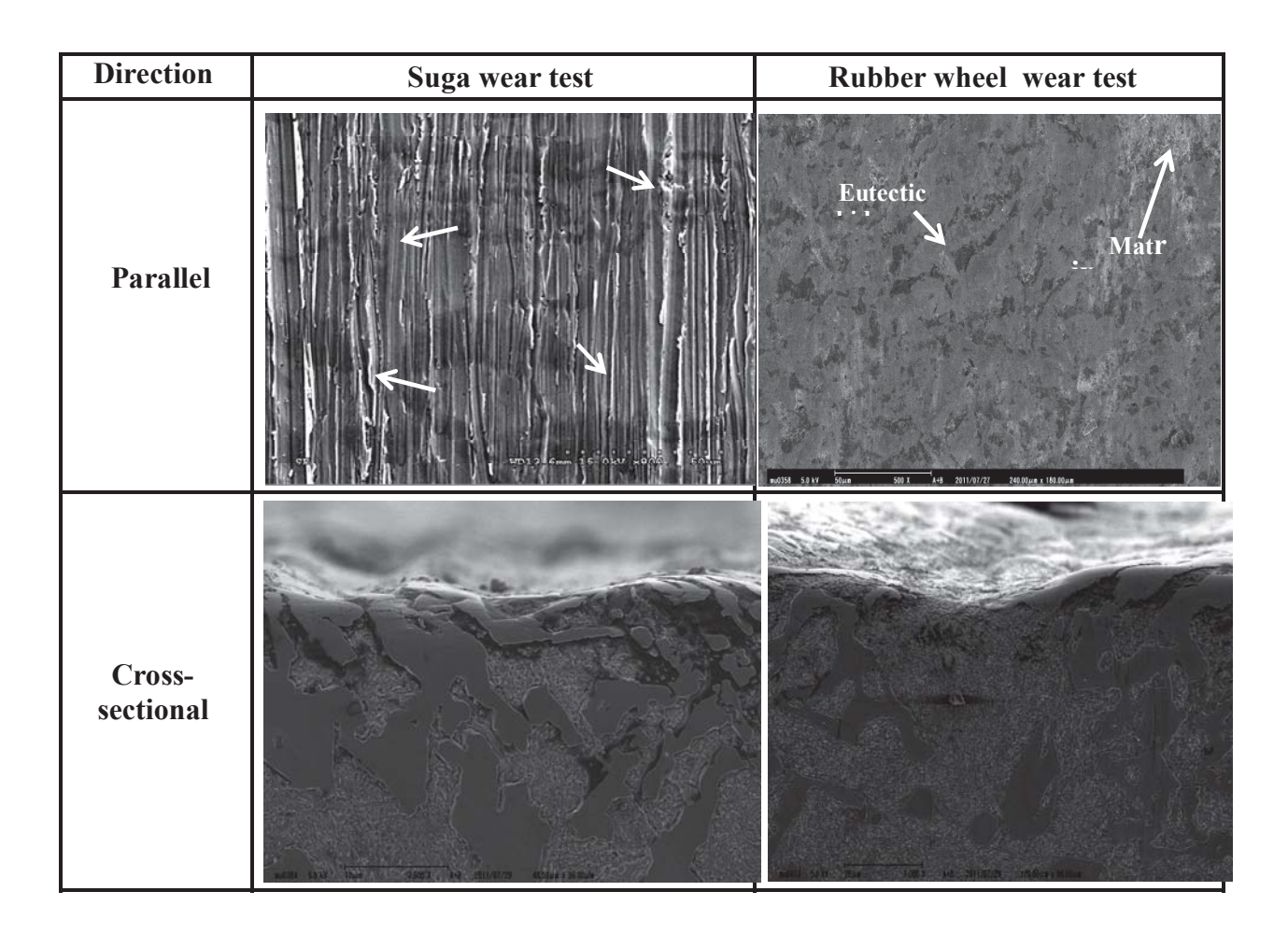


Fig. 4.18 Parallel and cross-sectional microstructures of worn surfaces of 1%Mo specimen with  $H_{Tmax}$ . (S: Scratching, G: Grooving, P: Pitting and T: Tearing.)

## Chapter 5

### **Conclusions**

The abrasive wear behavior of heat-treated hypocutectic 26% Cr cast irons without and with Mo was investigated. After annealing, the specimens were hardened from 1323 K and tempered at three levels of temperatures, the temperature giving the maximum hardness ( $H_{Tmax}$ ), and the lower and higher temperature than the  $H_{Tmax}$  temperature, (L- $H_{Tmax}$ , H- $H_{Tmax}$ ). The effects of hardness, volume fraction of retained austenite ( $V\gamma$ ) and the heat treatment conditions on the abrasive wear behavior were clarified. The following conclusions have been drawn from the experimental results and discussions.

- 1) The linear relationship was obtained between wear loss and wear distance in both of the two-body type Suga wear test and the three-body type Rubber wheel wear test. The highest wear resistance was obtained in the as-hardened or  $H_{Tmax}$  specimens. The lowest wear resistance was obtained in H- $H_{Tmax}$  specimen.
- 2) The Rw decreased with an increase in the hardness. The hardness had more effect on Rw in Suga wear test than that in Rubber wheel wear test.
- 3) The smallest  $R_W$  was obtained in the tempered specimen containing a certain quantity of retained austenite,  $10-15\%V_{\gamma}$ .
- 4) The Rw decreased gradually with increasing Mo content in Suga wear test. On the other hand, the Rw varies little by Mo addition in Rubber wheel wear test.
- 5) The macrohardness showed a strong effect on the Rw in Suga wear test. By contrast, matrix hardness or microhardness gave a major effect on the Rw in Rubber wheel wear test.
- 6) The matrix was preferably shaved off or worn off, and removed faster and more than the eutectic area. When this process continues, the cracks causes in the eutectic carbides, and resultanly, the spalling occurs and the eutectic carbides are removed.

### References

- [1] Laird, G., Gundlach, R., and Rohring, K. Abrasion-Resistance Cast Iron Handbook. USA: American Foundry Society, 2000.
- [2] Matsubara, Y., Ogi, K., and Matsuda, K. Eutectic solidification of high chromium cast ironeutectic structures and their quantitative analysis. AFS Transaction 89 (1981): 183-196.
- [3] Inthidech, S., Sricharoenchai, P., and Matsubara, Y. Effect of alloying element on heat treatment behavior of hypoeutectic high chromium cast iron. Materials Transactions 47 (2006): 72-81.
- [4] Sare, I.R., and Arnold, B.K. The effect of heat treatment on gouging abrasion resistance of alloy white cast iron. Metallurgical and Materials Transaction A 26A (1995): 357-370.
- [5] Kim, C. X-Ray method of measuring retained austenite in heat treat white cast irons. Journal of Heat Treating 1 (1979): 43-51.
- [6] Sudsakorn Inthidech. Heat Treatment Behavior of High Chromium Cast Iron for Abrasive Wear Resistance. Doctoral dissertation, Metallurgical Engineering, Faculty of Engineering, Chulalongkorn University, 2005.
- [7] Inthidech, S., Aungsupaitoon, P., Sricharoenchai, P., and Matsubara, Y. Two-body-type abrasion wear behavior in hypoeutectic 16 % Cr cast irons with Mo. International Journal of Cast Metal Research 23 (2010): 164-172.
- [8] Phasit Aungsupaitoon. Abrasion Wear Behavior of Hypoeutectic 16 Mass% Chromium Cast Iron Containing Molybdenum. Master's Thesis, Metallurgical Engineering, Faculty of Engineering, Chulalongkorn University, 2008.
- [9] Tabrett, C.P., Sare, I.R., and Ghomashchi, M.R. Microstructure-property relation in high chromium white iron alloys. International Materials Reviews 41 (1996): 59-82.
- [10] Davis, J.R. Metallurgy and Properties of High-Alloy White Irons. Cast Irons, pp. 107-122. Ohio: ASM International, 1996.
- [11] Ikeda, M., et al. Effect of molybdenum addition on solidification structure mechanical properties and wear resistivity of high chromium cast irons. ISIJ International 32 (1992): 1157-1162.
- [12] Thong, C.P., Suzuki, T., and Umeda, T. Eutectic solidification of high-chromium cast irons. Physical Metallurgy of Cast Iron IV (1989): 403-410.
- [13] Powell, G.L.F. Morphology of eutectic M<sub>3</sub>C and M<sub>7</sub>C<sub>3</sub> in white iron castings. Metals Forum 3 (1980): 37-46.
- [14] Dogan, Ö.N., Hawk, J.A., and Laird II, G. Solidification structure and abrasion resistance of high chromium white irons. Metallurgical and Materials Transactions A 28A (1997):

- 1315-1328.
- [15] Dogan, Ö.N. Effect of chemical composition and superheat on macrostructure of high Cr white iron castings. Abrasion 2005: An International Conference on Abrasion Wear Resistant Alloyed White Cast Iron For Rolling and Pulverizing Mills, Sao Paulo, Brazil, Aug. 14-17, 2005, 179-188. Sao Paulo: Escola Politecnica da USP, 2005.
- [16] Maratray, F., and Usseglio-Nanot, R. Factors affecting the structure of chromium and chromium-molybdenum white irons. Climax Molybdenum S.A. (1970): 10.
- [17] Laird II, G. Microstructure of Ni-hard I, Ni-hard IV and high-Cr white cast irons. AFS Transactions 99 (1991): 339-357.
- [18] Chung, R.J., et al. Effects of titanium addition on microstructure and wear resistance of hypereutectic high chromium cast iron Fe–25wt.%Cr–4wt.%C. Wear 267 (2009): 356-361.
- [19] He-Xing, C., Zhe-Chuan, C., Jin-Cai, L., and Huai-Tao, L. Effect of niobium on wear resistance of 15%Cr white cast iron. Wear 166 (1993): 197-201.
- [20] Tylczak, J.H., and Oregon, A. Abrasive wear. ASM Handbook 18 (1992): 337-351.
- [21] Chattopadhyay, R. Abrasion. Surface Wear: Analysis, Treatment, and revention, pp. 72-79. Ohio: ASM International, 2001.
- [22] Trope, W.R., and Chicco, B. The Fe-rich corner of the metastable C-Cr-Fe liquidus surface. Metallurgical Transactions A 16A (1981): 11-19.
- [23] Dupin, P., Saverna, J., and Schissler, J.M. A structural study of chromium white cast iron. AFS Trans 90 (1982): 711-718.
- [24] Bedolla-Jacudine, A. Microstructure of vanadium-, niobium,-and titanium-alloyed high-chromium white cast irons. International Journal of Cast Metals Research 13 (2001): 343-361.
- [25] Rickard, J. Some experiments concerning the as-cast grain size in 30% chromium cast irons. BCIRA Journal 8 (1960): 200-216.
- [26] Powell, G.L.F., Carlson, R.A., and Randle, V. The morphology and microtexture of M<sub>7</sub>C<sub>3</sub> in Fe-Cr-C and Fe-Cr-C-Si alloys of near eutectic composition. Journal of Materials Science 29 (1994): 4889-4896.
- [27] Laird, G., and Powell, G.L.F. Solidification and solid-state transformation mechanisms in Si alloyed high-chromium white cast irons. Metallurgical Transactions A 24A (1993): 981-988.
- [28] Matsubara, Y., Ogi, K., and Matsuda, K. Influence of alloying elements on the eutectic structures of high chromium cast iron. Journal of the Japan Foundrymen's Society

- (IMONO) 51 (1979): 545-550.
- [29] Tang, X.H., et al. Variations in microstructure of high chromium cast irons and resultant changes in resistance to wear, corrosion and corrosive wear. Wear 267 (2009): 116-121.
- [30] Liang, G.Y., and Su, J.Y. The effect of rare earth elements on the growth of eutectic carbides in white cast irons containing chromium. Cast Metals 4 (1991): 83-88.
- [31] Shen, J., and Zhou, Q.D. Solidification behavior of boron-bearing high-chromium cast iron and the modification mechanism of silicon. Cast Metals (1988): 79-85.
- [32] Pearce, J.T.H. Structure and wear performance of abrasion resistant chromium cast irons. AFS Transactions 92 (1984): 599-622.
- [33] Gunldlach, R.B., and Doane, D.V. Alloy cast irons. ASM Handbook 1 (1990): 222-268.
- [34] Sare, I.R., and Arnold, B.K. The influence of heat treatment on the high-stress abrasion resistance and fracture toughness of alloy white cast irons. Metallurgical Transactions A 26A (1995): 1785-1793.
- [35] Inthidech, S., et al. Behavior of hardness and retained austenite in heat treatment of high chromium cast iron for abrasive wear resistance. AFS Transaction (2004): 899-910.
- [36] Sare, I.R., and Arnold, B.K. The influence of heat treatment on the high-stress abrasion resistance and fracture toughness of alloy white cast irons. Metallurgical Transactions A 26A (1995): 1785-1793.
- [37] Powell, G.L.F., and Bee, J.V. Secondary carbide precipitate in an 18wt%Cr-1wt%Mo white iron. Journal of Materials Science 31 (1996): 707-711.
- [38] Maratray, F., and Poulalion, A. Austenite retention in high-chromium white iron. AFS Transactions 90 (1982): 795-804.
- [39] Stachowiak, G.W, and Batchelor, A.W. Engineering Tribology. USA: Elsevier, 2005.
- [40] Zum Gahr, K., and Doane, D.V. Optimizing fracture toughness and abrasion resistance in white cast irons. Metallurgical Transactions A 11A (1980): 613-620.
- [41] Watson, J.D., Mutton, P.J., and Share, I.R. Abrasive wear of white cast iron. Metal forum 3 (1980): 74-88.
- [42] Radulovic, M., Fiset, M., Peev, K., and Tamovic, M. The influence of vanadium on fracture toughness and abrasion resistance in high chromium white cast irons. Journal of Materials Science 29 (1994): 5085-5094.
- [43] Albertin, E., and Sinatora, A. Effect of carbide fraction and matrix microstructure on the wear of cast iron balls tested in a laboratory ball mill. Wear 250 (2001): 492-501.
- [44] Share, I.R. Abrasion resistance and fracture toughness of white cast irons. Metals technology 6 (1979): 412-419.